Title
Dendritic Spine Dynamics in Retrosplenial Cortex During Spatial Learning

Author
Frank, Adam

Publication Date
2015

Peer reviewed|Thesis/dissertation

UNIVERSITY OF CALIFORNIA

Los Angeles

Dendritic Spine Dynamics in Retrosplenial Cortex During Spatial Learning

A dissertation submitted in partial satisfaction

of the requirements for the degree

Doctor of Philosophy in Neuroscience

by

Adam Charles Frank

2015

ABSTRACT OF THE DISSERTATION

Dendritic Spine Dynamics in Retrosplenial Cortex During Spatial Learning

by

Adam Charles Frank

Doctor of Philosophy in Neuroscience

University of California, Los Angeles, 2015

Professor Alcino Jose Silva, Chair

Molecular and electrophysiological studies find convergent evidence suggesting that plasticity within a dendritic tree is not randomly dispersed, but clustered into functional groups. *In silico* neuronal modeling further suggests that clustered plasticity is able to increase storage capacity 45 times compared to dispersed plasticity. Recent *in vivo* work utilizing chronic two-photon microscopy tested this clustered plasticity hypothesis and showed that repetitive motor learning is able to induce clustered addition of new dendritic spines in primary motor cortex; moreover, clustered spines are more stable than non-clustered spines, suggesting a physiological role for spine clustering in learning. In this dissertation I further test the clustered plasticity hypothesis while also examining the spatial distribution of dendritic spine gain and loss. Additionally, I explore the hypothesis that spine turnover prior to learning is indicative of the plasticity within a neuronal network and thus impacts future learning and memory. To accomplish this, I utilized *in vivo* two-photon microscopy in Thy1-YFP-H mice to chronically image dendritic spine dynamics in retrosplenial cortex (RSC) during spatial learning. RSC is a key component of an extended spatial learning and memory circuit that includes hippocampus and entorhinal cortex. Importantly, RSC is known from lesion, immediate early gene expression, and optogenetic activation studies to be critically involved broadly in spatial learning

and more specifically in contextual fear conditioning. I thus utilized a modified contextual fear conditioning protocol that creates gradual increases in context freezing. Behavioral training was coupled with four *in vivo* imaging sessions that allowed me to examine spine dynamics before training, early in learning, and after animals had reached behavioral asymptote. Results from these studies show that contextual learning induces a significant increase in the formation of clusters of new dendritic spines and that the number of new clustered spines correlates with behavioral performance; specifically, animals with the highest proportion of new spines formed in clusters also have the highest context freezing. These results support the hypothesis that spine clustering is a general mechanism for learning-related information storage in the brain and a mechanism specifically operating in the RSC. Furthermore, I find that spines lost during learning preferentially occur near clustered new spines and that spine loss also correlates with memory. Finally, I find that spine turnover before learning correlates with future learning and with clustered spine addition. From these data, I propose a model where baseline spine turnover reflects the potential for a given animal to establish new synaptic contacts during learning and clustering represents a mechanism to stabilize these connections.

The dissertation of Adam Charles Frank is approved.

Dean Buonomano

Michael Fanselow

Kelsey Martin

Thomas O'Dell

Joshua Trachtenberg

Alcino Jose Silva, Committee Chair

University of California, Los Angeles

2015

Table of Contents

List of Figures

List of Tables

Acknowledgements

The work presented herein would not have been possible without the support of my advisor, Alcino Silva, whose guidance, advice, and input greatly influenced me as a graduate student throughout my time in his lab. I would also like to thank my thesis committee for their insightful advice and guidance— each committee meeting served to energize me intellectually and seed my mind with exciting new ideas to pursue. I am also grateful to the entire Silva Lab who contributed to discussions about the work, especially to Denise Cai, Justin Shobe, and Shan Huang. Furthermore, the Trachtenberg Lab was an invaluable resource while I learned two-photon imaging, especially Amos Gdalyahu. Finally, I would not be where I am today without the love, support and opportunities given to me by my parents, Charles and Margaret Frank; and without the love and support of my friends, family and most of all, my partner Lawrence Wong.

For funding I would like to thank the UCLA Medical Scientist Training Program (MSTP) and the UCLA Molecular and Cellular Training Program (2012; NIH Grant T32MH1938414).

Vita

EDUCATION

2003-2007	University of Pittsburgh, Pittsburgh, PA Bachelor of Science, Neuroscience, summa cum laude Bachelor of Arts, History and Philosophy of Science, summa cum laude

AWARDS & HONORS

2014	First Place, Best Poster Award Dendrites 2014 Conference, Crete
2012	Institutional Training Grant Fellow UCLA Molecular and Cellular Neuroscience Training Program
2009	Hagan-Schneider Medical Student Grant Southern California Lambda Medical Association
2008	MD-PhD Conference Travel Award NIMH/Society of Biological Psychiatry
2007	Bradler Award for Undergraduate Research University of Pittsburgh
2007	Phi Beta Kappa honor society
2006	OEL Small Grant Travel Award University of Pittsburgh
2004	Allison K. Bentley Biological Sciences Award Department of Biological Sciences, University of Pittsburgh
2003-2007	Honors Scholarship University of Pittsburgh

RESEARCH EXPERIENCE

7/2009 - Present	Graduate Student, University of California, Los Angeles PI: Alcino Silva, PhD Dendritic Spine Dynamics in Spatial Learning
7/2007-9/2007	Research Rotation, University of California, Los Angeles PI: William Yang, PhD BAC Models of Huntington's Disease
9/2003-6/2007	Undergraduate Research and Senior Thesis, University of Pittsburgh PI: Michael J. Palladino, PhD Drosophila Models of Mitochondrial Encephalomyopathy

PUBLICATIONS

1. Thomas Rogerson, Denise J. Cai, **Adam C. Frank**, Yoshitake Sano, Manuel F. Lopez-Aranda, Alcino J. Silva. Synaptic tagging during memory allocation. Nature Reviews Neuroscience, 15, 157-169 (2014).

2. Alicia M. Celotto, **Adam C. Frank**, Steven W. McGrath, Timothy J. Fergestad, Wayne A. Van Voorhies, Karolyn Buttle, Carmen A. Mannella and Michael J. Palladino. Mitochondrial Encephalomyopathies in *Drosophila*. The Journal of Neuroscience, January 18, 2006. 26(3):810–20.
3. Alicia M. Celotto, **Adam C. Frank**, Jacquelyn L. Seigle, and Michael J. Palladino. Drosophila Model of Human Inherited Triosephosphate Isomerase Deficiency Glycolytic Enzymopathy. Genetics, November 15, 2006. 174(3): 1237-46.

TALKS

1. **Adam C. Frank**, Amos Gdalyahu, Joshua T. Trachtenberg, Alcino J. Silva (2013). Contextual Learning Induces Changes in Dendritic Spine Stability and Spine Clustering in Retrosplenial Cortex. 12th Annual Molecular and Cellular Cognition Society Meeting.

ABSTRACTS

1. **Adam C. Frank**, Amos Gdalyahu, Joshua T. Trachtenberg, Alcino J. Silva (2014). Contextual Learning Induces Dendritic Spine Clustering in Retrosplenial Cortex. Frontiers in Systems Neuroscience, DOI: 10.3389/conf.fnsys.2014.05.00021
2. **Adam C. Frank**, Denise J. Cai, Alcino Silva (2012). BAC transgenic chemical-genetic overexpression of alpha-CaMKII generates reversible memory deficits. 42nd Annual Society for Neuroscience Conference.
3. **Adam C. Frank**, Amos Gdalyahu, Joshua T. Trachtenberg, Alcino J. Silva (2014). Contextual Learning Induces Changes in Dendritic Spine Stability and Spine Clustering in Retrosplenial Cortex. 43rd Annual Society for Neuroscience Conference.
4. Justin L. Shobe, Denise J. Cai, **Adam C. Frank**, Tristan Shuman, Karsten Baumgaertel, Kiriana K. Cowansage, Jeremy Biane, Mark Mayford & Alcino J. Silva (2011). Testing the Behavioral Implications of Memory Allocation. 41st Annual Society for Neuroscience Conference.
5. Anthony Landreth, Tawnie Silva, Mika Guzman, Anna Matynia, Miou Zhou, **Adam C. Frank**, Alcino Silva (2009). A reverse genetic screen for novel memory mutants. 39th Annual Society for Neuroscience Conference.
6. Michael J. Palladino, **Adam C. Frank,** Jacquelyn L. Seigle, Alicia M. Celotto (2007). *Drosophila* model of human inherited TPI deficiency glycolytic enzymopathy. 48th Annual Drosophila Research Conference.
7. Michael J. Palladino, **Adam C. Frank**, Nicole M. Kotchey, Alicia M. Celotto (2007). Mitochondrial Encephalomyopathy in *Drosophila*: Pathogenic Mechanisms and Therapeutic Approaches. 48th Annual Drosophila Research Conference.
8. **Adam C. Frank**, Steven W. McGrath, Alicia M. Celotto, and Michael J. Palladino (2006). Mitochondrial Encephalomyopathies in *Drosophila*. 47th Annual Drosophila Research Conference.
9. Christian Renken, Karolyn F. Buttle, Michael Marko, Chyong-Ere Hseih, **Adam C. Frank**, Michael J. Palladino, Carmen A. Mannella (2006). Topology of the Mitochondrial Inner Membrane. Biophysical Society Meeting.
10. **Adam C. Frank**, Steve W. McGrath, Alicia M. Celotto and Michael J. Palladino (2005). Mitochondrial encephalomyopathies in Drosophila. Science 2005.

Chapter 1

Introduction

Great strides have been made within the past half century towards elucidating structural, biochemical, and electrical properties of neurons that allow the brain and nervous system to retain information in the service of learning and memory formation. Studies of long term potentiation (LTP) form the cornerstone of our understanding of learning-related changes that occur within neurons (Miller and Mayford, 1999). However, a variety of other mechanisms, such as branch-specific potentiation and clustered spine addition, have recently been discovered that also impact information storage in the nervous system (Losonczy et al., 2008; Fu et al., 2012). While our understanding of how information is retained is advancing, still in its infancy is our understanding of where these changes occur. However, a theme has emerged from the data: plastic changes to neurons do not occur randomly throughout the dendritic tree, but rather are concentrated together in functionally related clusters (Govindarajan et al., 2006). Formalized as the clustered plasticity model, this conceptual framework is supported by data from a variety of fields in neuroscience and has helped to foment more directed efforts towards understanding this complicated problem.

A number of studies have found evidence for clustered plasticity and have begun to elucidate the processes that govern this phenomenon. Results from both *ex vivo* and *in vivo* studies of LTP have uncovered a number of biochemical processes and molecules that interact to generate clustered plasticity. Electrophysiological experiments have also shown that dendrites and dendritic spines are capable of carrying out complex calculations locally, in a

manner that can both influence induction of clustered plasticity and also make use of electrical properties established due to clustered plasticity. Furthermore, a number of studies have carefully examined neuronal and dendritic morphology and found evidence of clustered structural plasticity. Finally, these studies are unified by theoretical and computational work that suggests a framework for understanding why plastic events are spatially clustered within a neuron.

1.1 Biochemical Studies of Clustered Plasticity

Several studies have found biochemical evidence of clustered plasticity (Govindarajan et al., 2011; Harvey and Svoboda, 2007; Harvey et al., 2008; Murakoshi et al., 2011; Makino and Malinow, 2011). First, Harvey *et al* in a series of studies found both evidence of and a mechanism for a time- and space-dependent facilitation of LTP (Harvey and Svoboda, 2007; Harvey et al., 2008). Specifically, utilizing two-photon glutamate uncaging in hippocampal slices, the authors were able to induce NMDA receptor (NMDAR)- dependent LTP at single dendritic spines, measured as both an increase in micro-excitatory post-synaptic current (μEPSC) and spine head volume. Importantly, this LTP induction protocol was site specific as nearby spines did not experience a calcium influx during glutamate uncaging or a change in spine head volume following stimulation. Weak stimulation of a spine with low levels of glutamate uncaging had no effect on either μEPSC size or spine head volume. Strikingly, if, following LTP induction at one spine, a weak stimulation was applied to a nearby spine, this spine also experienced an increase in μEPSC and spine head volume. The authors deemed this phenomenon “crosstalk,” and found that it occurred when weak stimulation occurred within 10 minutes of LTP induction and within approximately 10 microns (μm) of the stimulated spine.

Excitingly, the authors proceeded to demonstrate that the diffusible molecule H-ras had properties and kinetics that allowed it to facilitate this “crosstalk” phenomenon between spines.

First, H-ras is specifically activated by LTP-inducing glutamate uncaging. Second, activated H-ras is able to diffuse out of the stimulated dendritic spine, travel approximately 10 μm along the dendritic shaft, and diffuse into nearby neighboring spines. Finally, spine "crosstalk" is significantly attenuated if an inhibitor of MEK, a downstream target of ras activity, is applied after LTP induction but before subthreshold activation of a neighboring spine. With this elegant series of experiments the authors demonstrate that Ras activation and diffusion is a key component of interactions between nearby spines during plasticity events, providing biochemical support for the clustered plasticity model.

In a related series of experiments, Murakoshi *et al* demonstrate that two diffusible Rho-GTPases – RhoA and Cdc42 - are important for spine volume increases following LTP induction (Murakoshi et al., 2011). Specifically, LTP induction at single spines was again accomplished via two-photon glutamate uncaging. RhoA and Cdc42 were rapidly activated in the stimulated spine and remained active here for approximately 25 minutes. While Cdc42 remained largely confined to the stimulated spine, RhoA was able to diffuse out into the dendritic shaft, travel approximately 5 μm, and invade nearby spines. If activity of either RhoA or Cdc42 was blocked, spine volume changes were abrogated. While the authors did not directly address the question of plasticity crosstalk between neighboring spines, it is possible that RhoA plays a similar and related role as H-Ras in facilitating plasticity induction between nearby spines, especially given that blockade of H-Ras activity does not completely abolish increases in spine volume at neighboring spines (Harvey et al., 2008).

Activation and diffusion of a variety of GTPases is one mechanism that regulates where plastic events occur and promotes formation of clusters of plastic changes (i.e. induction of LTP at one synapse facilitates induction of LTP at a nearby synapse). However, Govindarajan *et al* demonstrate that local protein synthesis is another mechanism involved in clustered plasticity, and one which operates over longer temporal and spatial scales (Govindarajan et al., 2011). Specifically, the authors sought to better understand the spatial dynamics of the synaptic tag

and capture (STC) model of plasticity. This model states that 1) synapses receiving both weak and strong input are tagged in a protein synthesis-independent manner; 2) only strong input is able to induce synthesis of plasticity-related proteins; and, 3) plasticity-related proteins can be captured at any synapse that has been tagged. The authors, working in hippocampal slices, made use of two-photon glutamate uncaging in the presence of forskolin (a protein kinase A agonist) as a strong stimulus capable of inducing protein synthesis-dependent long-LTP (L-LTP). This protocol was capable of inducing long lasting increases in both μEPSC size and spine volume specifically on the stimulated spine. Weak stimulation was carried out by glutamate uncaging in the absence of forskolin (with a lack of volume increase observed at the stimulated spine).

The authors demonstrate the power of their system by replicating findings from classical STC experiments. First, strong stimulation (glutamate+forskolin) of one spine induced L-LTP at the stimulated spine and induced translation of plasticity-related proteins. These proteins could then be captured by a nearby synapse to convert early-LTP (E-LTP) to L-LTP, whether the neighboring synapse was given a weak stimulation (glutamate alone) or a strong stimulation in the presence of a protein synthesis inhibitor. Further, tag setting and E-LTP induction at one synapse via weak stimulation could be converted to L-LTP due to plasticity-related proteins generated at a later time point due to L-LTP induction at a second synapse. As mentioned, the time course of rescue of E-LTP to L-LTP is longer than for synaptic “crosstalk” due to sharing of active GTPases, and is on the order of one to two hours. Strikingly, though, the authors found that distance between stimulated spines was still an important factor for facilitation of plasticity. Specifically, a weakly stimulated spine was able to undergo L-LTP (i.e. capture plasticity-related proteins) if the strongly stimulated spine was within a distance of approximately 70 μm on the same dendritic branch. Surprisingly, rescue of L-LTP was much less efficient if the two stimulated spines were on sister branches of the same dendrite. In this case, capture of

plasticity-related proteins occurred up to a distance of approximately 45 μm, suggesting the existence of a mechanism to limit protein spread between dendritic compartments.

The evidence from these aforementioned studies suggests that there are multiple biochemical mechanisms in place that regulate where and when plastic events occur within dendrites and how they interact. Activation and diffusion of GTPases occurs and returns to baseline quickly, within tens of minutes. Further, diffusion of activated GTPases is restricted to a domain of 5-10 μm from the stimulated spine, which restricts facilitation of LTP to neighboring spines within this spatial window. Sharing of plasticity-related proteins via synaptic tag and capture, however, occurs over a longer time scale, on the order of one to two hours, and over distances of tens of microns. At this spatial scale, it was also observed that distance alone is not the only factor governing the sharing of plasticity-related proteins, but that the branch point between dendrites acts as a filter to further limit diffusion of newly synthesized proteins. Finally, though these two mechanisms operate over different temporal and spatial domains, it is likely that they interact with each other. As a hypothetical example, assume a strong stimulus impinges on one spine (Spine A) and is sufficient to activate H-ras, tag the spine, and induce local translation of plasticity-related proteins (Figure 1.1). Now examine two nearby spines: Spine B is 10 μm away from Spine A and receives a weak input five minutes after the strong stimulation. Being close enough to the strongly stimulated spine to share in activated H-ras and thus experience a reduction in the threshold for LTP, Spine B is able to undergo not only E-LTP and receive a tag, but is then able to convert this E-LTP to L-LTP by capturing the previously synthesized plasticity-related proteins. The second nearby spine, Spine C, is also 10 μm away but receives a weak input 30 minutes after the strong stimulation to the first spine. No changes occur to Spine C, however, as the activity of H-ras induced by strong stimulation of spine one has returned to baseline. This means that the weak stimulation of this neighboring spine is not sufficient, in the absence of active H-ras, to generate E-LTP, no synaptic tag is set, and thus no plasticity-related proteins are captured.

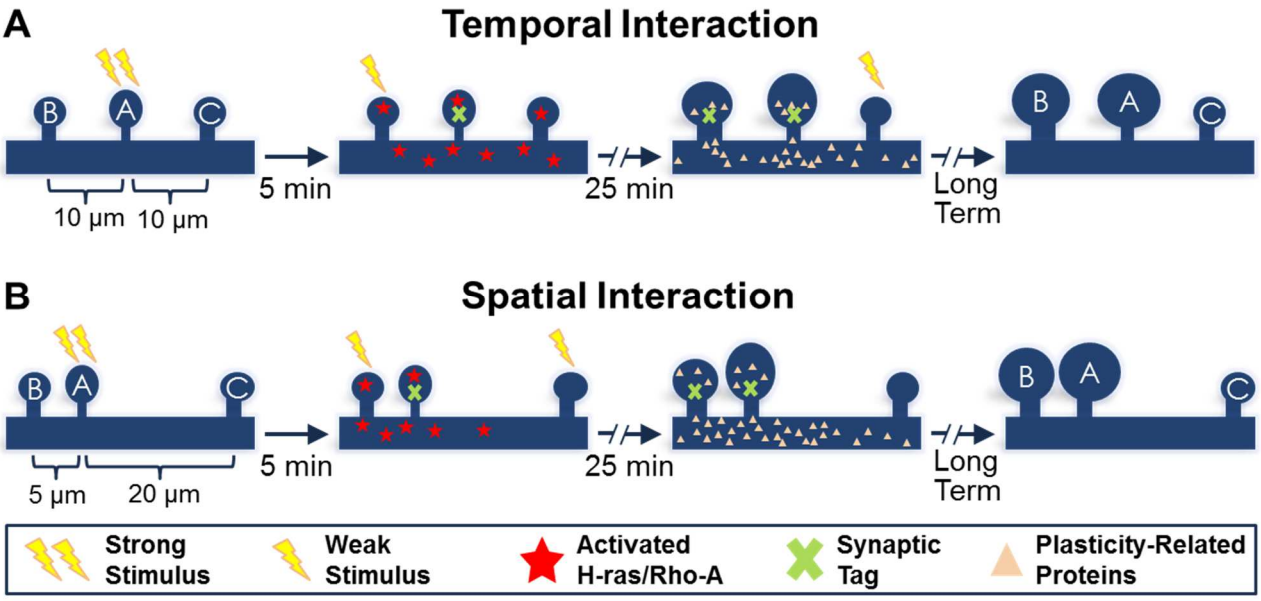

Figure 1.1: Hypothetical temporal and spatial interaction of synaptic crosstalk with synaptic tag-and-capture. (A) Three neighboring dendritic spines receive temporally distinct inputs of variable intensity. Spine A receives a strong, L-LTP inducing stimulus first, followed 5 minutes later by a weak stimulus at Spine B. Spine B has a lower threshold for LTP induction due to H-ras and/or Rho-A crosstalk from Spine A and thus experiences E-LTP and synaptic tag setting. Spine B is now able to capture plasticity related proteins generated due to the strong stimulation of Spine A; and both Spine A and Spine B undergo L-LTP and have an increase in spine head volume. Spine C receives a weak input 30 minutes after that at Spine B; and this input, being outside the synaptic crosstalk temporal window does not allow for a reduction in LTP threshold at Spine C, which does not under E-LTP, tag setting, protein capture, or L-LTP. (B) Two neighboring and one distant spine receive inputs closely spaced in time. As in (A), Spine A receives a strong, L-LTP inducing stimulus first, followed 5 minutes later by a weak stimulus at both Spine B and Spine C. Spine B is within the spatial window for synaptic crosstalk and thus has a lowered threshold for LTP induction due to sharing of activated H-ras and/or Rho-A from Spine A. Spine B is then able to undergo E-LTP, tag setting, capture of plasticity related proteins, L-LTP, and spine volume increase. Spine C is outside of the spatial window for synaptic crosstalk and thus does not experience any changes due to weak stimulation alone.

While this example demonstrates the importance of temporal dynamics in sharing of plasticity resources, a similar argument for interaction between shorter (i.e. GTPase activation/diffusion) and longer (synaptic tag and capture) spatial mechanisms of clustered plasticity could be made. As another example, Spine A receives a strong, L-LTP inducing stimulus while Spine B and Spine C are stimulated with the same amount of weak input at the same time, 5 minutes later. However, Spine B is 5 µm away from the strongly stimulated Spine A, while Spine C is 20 µm away. Here again Spine B would be able to take advantage of both the diffused, activated H-ras to undergo E-LTP and tag generation and subsequently capture

plasticity-related proteins. Again, Spine C would experience neither of these effects due to its distance from the strongly stimulated spine.

Excitingly, *in vivo* work has added new complexity to the biochemical processes that govern clustered plasticity. Specifically, Makino and Malinow utilized a green fluorescent protein (GFP)-tagged version of the GluR1 AMPA receptor (AMPAR) subunit to track where plasticity occurred in the barrel cortex (Makino and Malinow, 2011). As GluR1 insertion is required initially and temporarily for LTP generation, this system allowed the authors to determine where plasticity had recently occurred within a narrow time window. Experimental animals expressed Cre-recombinase under control of 4-hydroxytamoxifen (4-OHT) and were electroporated *in utero* with the GluR1-GFP construct which had a floxed stop codon at the 5' end of the gene to prevent spurious expression. At postnatal day 11 the animals were injected with 4-OHT to allow expression of Cre which subsequently removed the stop codon from the GluR1-GFP construct to allow for expression of the tagged AMPAR subunit. Animals were given two days to experience natural whisker stimulation in their cages and then sections of the barrel cortex were taken for two-photon imaging to assess the pattern and extent of GluR1-GFP expression. To begin, the authors validated their experimental system by demonstrating that GluR1-GFP expression levels are significantly higher in animals with intact whiskers versus animals whose whiskers had been trimmed. Next, the authors asked whether there was a subcellular spatial pattern to the enrichment in GluR1-GFP expression in spines in whisker-intact animals. Strikingly, the authors found a significant positive correlation between enrichment of expression in neighboring spines. All spines from a given neuron were examined and only the highest 15% of enriched spines were analyzed, the authors found that the number of spine pairs that showed this enrichment was significantly above chance levels. Work by Zhang *et al* demonstrated similar results by tracking changes to AMPAR expression in spines in barrel cortex following whisker stimulation (Zhang et al., 2015). Here, the authors found that an increase in AMPAR receptor expression in one spine biased neighboring spines toward having

increases as well. Further, decreases in AMPAR expression in one spine biased neighboring spines to also having a decrease. In sum these results confirm findings from *ex vivo* studies demonstrating that biochemical processes related to synaptic plasticity show subcellular organization, more specifically these processes are clustered together and expressed in dendritic spines neighboring each other.

1.2 Electrophysiological Studies of Clustered Plasticity

In addition to biochemical interactions facilitating clustered plasticity, there are also numerous examples of electrophysiological interactions within dendrites that either demonstrate clustered plasticity, suggest mechanisms through which clustered plasticity might act, or influence the ability of clustered plasticity to occur (Larkum and Nevian, 2008). First, Takahashi *et al* found evidence of clustered co-activation of dendritic spines both in hippocampal slices and intact barrel cortex (Takahashi et al., 2012). Specifically, the authors monitored spontaneous calcium events in dendritic spines of CA3 pyramidal cells in hippocampal slices and found that following a calcium event at one spine, there was a greater-than-chance likelihood of witnessing a second calcium event within 100 milliseconds (ms) and within 8 μm of the original spine. The authors defined an assemblet as a group of co-active spines where the distance from any one spine to the next was within 10 μm. Strikingly, using this definition, they found that 31.5% of spines participated in at least one assemblet and that assemblet activity accounted for 29.5% of total spine activity. In single assemblet events, 2 to 12 spines were activated (on average 3.6 ± 0.7 spines) during a period of 59 ± 33 ms and within a distance of 4.7 ± 3.3 μm. The authors found that assemblet size and number of repetitions of assemblet activation were greater than the chance values one would expect by event-interval shuffling. Interestingly, assemblet organization and emergence was dependent on local plasticity as assemblets were less frequently seen in slices cultured in the presence of AP5, and NMDAR

antagonist, or in immature slices. Finally, the authors used two-photon microscopy to image dendritic spine calcium events in layer 2/3 neurons in intact mouse barrel cortex and found an increase in co-activity when spines were located within 6 μm of each other. Similar results by Kleindeinst *et al* in the developing hippocampus demonstrate that synapses on CA3 pyramidal cells located within 16 μm of each other were more likely to be co-active than synapses separated by greater distances (Kleindeinst et al., 2011). Taken together, these results suggest that spines located near each other are more likely to be co-active, suggesting they may transmit similar information.

A number of electrophysiological studies suggest properties of dendrites that can interact with clustered plasticity. First, Gasparini *et al* studied the properties of dendritic spikes in CA1 pyramidal neurons (Gasparini et al., 2004). Dendritic spikes are regenerative voltage spikes that can be initiated locally in dendrites and have the ability to propagate to the soma and initiate an action potential (Spruston, 2008). The authors found that perfusion of TTX onto hippocampal slices abolished dendritic spike generation, suggesting a role for Na^+ currents. Furthermore, spike threshold and amplitude were found to be dependent on A-type K^+ currents, such that blockade with 4-AP, a K^+ channel antagonist, both decreased spike threshold and increased spike amplitude. Additionally, the authors examined the spatiotemporal requirements for synaptic inputs on CA1 dendrites to cause dendritic spike generation. Inputs spaced 0.1 ms apart were most effective in inducing spike generation. Using this data, the authors then modeled multiple synaptic inputs spaced over a region of dendrite and found that highly synchronous inputs (approximately 50 synapses activated within 3 ms) with moderate clustering (all inputs impinging onto the dendrite within 100 μm) were most effective at eliciting dendritic spiking. These results suggest that clustered inputs could allow dendrites to act as efficient coincident detectors, adding a computational level to individual neurons.

At least two forms of plasticity are also influenced and governed by clustered input and dendritic spiking: LTP generation due to dendritic spikes and branch strength potentiation. First,

it has been known that a variety of depolarizing events, such as backpropagating action potentials (bAPs) (Magee and Johnston, 1997) and dendritic spikes (Remy and Spruston, 2007), are capable of generating LTP. What is striking is that synaptic stimulation paired with dendritic spikes is the most effective means to induce LTP in CA1 pyramidal cells (Hardie and Spruston, 2009). Further, Hardie *et al* also found that spatially restricted synaptic inputs provided greater increases in potentiation than did spatially distributed inputs, suggesting that closely spatiotemporally spaced activity in dendrites is one of the most efficient mechanisms for induction of plasticity.

The second form of plasticity that operates in a clustered, spatially restricted manner differs in kind from that of classical LTP. To begin, Losonczy *et al* utilized multi-site two-photon glutamate uncaging in basal and radial oblique dendrites of CA1 pyramidal cells, allowing them to deliver spatially clustered and temporally synchronous synaptic inputs that were capable of producing dendritic spikes (Losonczy et al., 2008). Interestingly, the authors found heterogeneity in the population of dendritic branches they sampled: most branches (78%) had dendritic spikes that lacked a large, fast voltage component (i.e. no initial large dV/dt) and which also attenuated within 20-40 μm from the site of generation. A minority of branches (22%) had large, fast voltage components to their dendritic spikes and also experienced no attenuation in spike size as they propagated toward the soma. This minority of strong branches had a disproportionately large influence on action potential generation as the fast spike component from strong branches was typically large enough to evoke action potential (AP) output with only approximately 55% of the input required compared to weak branches. The authors focused on proximal dendrites and found that 75% of primary proximal dendrites were strong, while a much smaller proportion of terminal branches (18%) displayed this property. In fact, when two daughter dendritic branches bifurcated from the same strong parent dendrite, the authors found that typically only one of the branches also displayed the strong dendritic spiking property of the parent and possessed large enough dendritic spikes to cause parent branch spiking. This

demonstrates that the system is set up to have local regulation of the strength and effect of synaptic input. However, even more striking is the fact that the strength of weak branches is modifiable. The authors use either local dendritic spike initiation paired with carbachol or theta stimulation paired with backpropagating action potentials and found they were able to induce a robust, but slowly developing enhancement in weak branch spike strength, which they termed branch strength potentiation. This enhancement was long lasting as it persisted after carbachol washout and was dependent on muscarinic acetylcholine receptors (mAChR) as well as NMDARs. The authors found that A-type K^+ currents were a main effector of the ability of dendritic spikes to propagate as low concentrations of Ba^+, known to block A-type K^+ channels, were able to enhance dendritic spike propagation from weak branches. This effect was only maintained while Ba^+ was present, in contrast to their results of spike enhancements due to carbachol application. The authors postulated that branch strength potentiation was thus due to a slow down regulation of A-type K^+ channels in the initially weak daughter branches. Excitingly, branch strength potentiation has also been shown to occur *in vivo* in rat CA1 following housing in enriched environments (Makara et al., 2009). Branch strength potentiation thus adds a unique form of plasticity, distinct from classical forms of synaptic weight changes, to the list of dendritic modifications that occur in a localized, clustered manner.

It should be mentioned that not all electrophysiological studies find support for clustered plasticity. In fact, three studies from the Konnerth group demonstrate a lack of spatially and temporally coordinated synaptic input in multiple sensory cortices. In the first, the authors found that layer 2/3 neurons in mouse primary visual cortex received orientation specific afferent inputs that were disbursed throughout the entire dendritic tree (Jia et al., 2010). Even for neurons with high orientation selectivity, a wide range of orientation inputs were received. Similar results were obtained for layer 2/3 neurons in mouse primary auditory cortex where frequency tuned neurons had dendritic spines with optimal response frequencies intermixed on the same segment of dendrite (Chen et al., 2011). Finally, layer 2/3 neurons in mouse barrel

cortex were analyzed by similar methods; calcium events occurred in dendritic spines throughout the dendritic tree and events triggered by principal and surround whisker stimulation were intermixed (Varga et al., 2011). In each region of sensory cortex the authors found evidence of a lack of synaptic inputs that were temporally and spatially synchronous and also similarly sensitive to stimulus parameter, which suggests that, at least in the sensory cortex and cell type examined, clustering of inputs, and by extension clustered plasticity, may not operate. An interesting question for futures studies is whether certain stimuli or stimulus characteristics are encoded through clustered input while others are not. Further, exploration of cell-type and region-specific evidence for and against clustered input will be important, as it is possible that certain excitatory neuronal types in specific brain regions preferentially use clustered versus non-clustered input modes.

In sum, one can envision all of the aforementioned biochemical and electrophysiological processes interacting to generate highly localized changes within the dendritic tree. As mentioned, diffusion of activated GTPases such as H-ras and Rho-A allow for nearby spines to experience a decrease in the threshold for LTP induction. This time-limited resource can be coupled with the sharing of locally synthesized plasticity-related proteins, which are available for use within a dendritic branch for an extended period of time, to extend E-LTP to L-LTP. Both forms of plasticity require induction of LTP, which could be generated locally due to dendritic spiking. Further, the ability of potentiated synapses on a given segment of dendrite to influence somatic potential and action potential generation could be modified locally due to repeated stimulation of the same synaptic inputs and the induction of branch strength potentiation.

1.3 Structural Plasticity and Dendritic Spines

Studies of structural plasticity, which have largely focused on changes to dendrites and dendritic spines, have also found evidence for clustered plasticity. A brief introduction to

structural plasticity provides a template of understanding for studies of clustered structural plasticity. To start, dendritic spines are small protrusions that emanate from the shafts of dendrites (McGuire et al., 1984). The majority of excitatory synapses within the cortex occur on dendritic spines and are formed through contact with *en passant* boutons (Spruston, 2008; Holtmaat and Svoboda, 2009). Usually one axonal bouton and one spine correspond to a single synapse, characterized by the presence of a presynaptic active zone with vesicles, a synaptic cleft separating pre- and post-synaptic elements, and an electron-dense postsynaptic density (PSD) (Harris et al., 1992; Colonnier, 1968; Shepherd and Harris, 1998). A minority of boutons and spines lack synapses and a small proportion of boutons participate in multiple synapses (Shepherd and Harris, 1998; Spacek, 1982; Arellano et al., 2007; Trachtenberg et al., 2002, Knott et al., 2006). Light and electron microscopy (EM) reconstructions of dendritic spines demonstrate that these structures come in a variety of morphologies and sizes with head diameters ranging from 0.001μm to 1 μm (Schallert et al., 2000; Peters and Kaiserman-Abramof, 1970; Harris and Stevens, 1989; Ballesteros-Yanez et al., 2006). Three classically defined spine shapes are the filopodia-like protrusion ('thin spine'), the short spine lacking a defined neck region ('stubby spine'), and the spine having both a defined neck region and a large head ('mushroom spine') (Peters and Kaiserman-Abramof, 1970; Harris and Kater, 1994).

Studies of dendrites and dendritic spines classically made use of techniques - such as EM and Golgi staining - that required sacrifice of the animal. Thus only a static image of the state of dendritic spines could be acquired and any comparisons had to be made at the group level (i.e. spine density in young animals versus adult animals). More recently, the use of two-photon *in vivo* imaging of transgenic and virally infected animals expressing fluorescent reporter proteins has allowed for the tracking of spine dynamics across time within the same animal. While large scale growth and retraction of the dendritic tree of adult cortical neurons is rarely seen (Holtmaat et al., 2005; Lee et al., 2006; Chow et al., 2009; Mizrahi and Katz, 2003), even following learning (Mizrahi and Katz, 2003) and environmental enrichment (Holtmaat et al.,

2005), small changes in the length of the branch tips of pyramidal cell dendrites have been observed (Holtmaat and Svoboda, 2009). More dynamic, however, is the location, size, and shape of dendritic spines. During early postnatal development the rate of gain and loss of dendritic spines is greater than any other period in an animal's life (Lendvai et al., 2000; Holtmaat et al., 2005; Zuo et al., 2005a). Spine density is also highest at this early postnatal age and begins to decrease as animals age (Holtmaat et al., 2005; Zuo et al., 2005a), which is consistent with classical work in primate and rodent cortex (Rakic et al., 1986; De Felipe et al., 1997). In the adult mouse, spine turnover continues, but at a greatly reduced rate relative to that during early postnatal development (Holtmaat et al., 2005; Zuo et al., 2005a; Trachtenberg et al., 2002; Grutzendler et al., 2002; Majewska et al., 2006). The lifetime of spines varies greatly, even in adulthood. Generally, spines that appear in the adult are likely to be eliminated within several days and are typically referred to as transient spines (Trachtenberg et al., 2002; Holtmaat et al., 2005; Grutzendler et al., 2002; Holtmaat and Svoboda, 2009). However, a small proportion of new spines will persist for over a week, and long term chronic imaging studies have found that these spines, referred to as persistent spines, are then likely to survive for months (Holtmaat et al., 2005; Zuo et al., 2005a; Holtmaat and Svoboda, 2009). *In vivo* imaging studies have broadly found that spine shape and size correlate with spine stability: small, thin spines are generally transient while large, mushroom spines are typically persistent (Majewska et al., 2006; Zuo et al., 2005a; Grutzendler et al., 2002). These findings are not, however, absolute as some small spines are found to make synapses and be persistent while some large spines are transient (Trachtenberg et al., 2002; Knott et al., 2006; Harris and Stevens, 1989; Nägerl et al., 2007; Fiala et al., 1998; Holtmaat and Svoboda, 2009).

The question of how formation and elimination of dendritic spines, which are visible with high resolution optical imaging, correlates to synapse formation requires additional techniques beyond light microscopy to address. Retrospective analysis using EM and array tomography in addition to direct imaging of synaptic proteins in vivo have allowed some insight into this

problem (Trachtenberg et al., 2002; Knott et al., 2006; Holtmaat et al., 2006; Zito et al., 1999; Zito et al., 2009; Micheva and Smith, 2007). Specifically, EM analysis of structures previously followed over days to weeks utilizing chronic *in vivo* imaging revealed that new spines could bear synapses (Trachtenberg et al., 2002; Holtmaat et al., 2006; Knott et al., 2006). Time-course analysis showed that all spines older than 4 days had synapses, while only 30% of spines that were two days old had a synapse (Knott et al., 2006). The remaining 70% of young spines have been postulated to correspond to a small steady-state population of spines that lack synapses (Spacek, 1982; Arellano et al., 2007). Interestingly, new spines have been found to preferentially form synapses with axonal boutons that already bear a synapse, resulting in multiple-synapse boutons (MSBs) (Knott et al., 2006; Nägerl et al., 2007; Toni et al., 2007). Strikingly, approximately 65% of new spines in somatosensory cortex (Knott et al., 2006), cultured hippocampal slices (Nägerl et al., 2007), and dentate gyrus (Geinisman et al., 2001) form synapses on MSBs, which suggests that formation of synapses on MSBs is a common mechanism for structural plasticity in the adult brain (Holtmaat and Svoboda, 2009).

Classical techniques coupled with *in vivo* imaging have allowed for exploration of how experience impacts spine dynamics. While baseline turnover in the adult mouse is generally consistent throughout life, a variety of manipulations have been shown to impact spine gain, spine loss, and spine density. For example, spatial learning (Moser et al., 1994), complex tone fear conditioning (Moczulska et al., 2013), rearing and training in enriched environments (Greenough et al., 1985; Beaulieu and Colonnier, 1987; Kolb et al., 2008; Jung and Herms, 2012), long-term sensory stimulation (Knott et al., 2002) and sensory deprivation (Zuo et al., 2005b) have all been shown to increase spine density in diverse cortical regions. Further, spine turnover rate and spine addition have been shown to be increased in frontal cortex after tone fear extinction (Lai et al., 2012), in barrel cortex following whisker trimming (Trachtenberg et al., 2002; Holtmaat et al., 2005), in visual cortex following monocular deprivation (Hofer et al., 2009; Yu et al., 2011) and retinal lesion (Keck et al., 2008), and in motor cortex following motor

learning (Xu et al., 2009). Finally, Lai *et al* found an increase in the rate of spine loss in frontal cortex due to tone fear conditioning (Lai et al., 2012). Excitingly, many of these studies have found that changes to spine dynamics correlate with functional alterations in neural circuitry and with learning. Specifically, following retinal lesion, the corresponding zone of visual cortex loses function temporarily; as function is recovered over one to two months due to invasion of neighboring visual areas, nearly all dendritic spines are replaced in this region (Keck et al., 2008). Additionally, animals' improvement on a seed-reaching task positively correlates with spine addition in the corresponding forepaw region of primary motor cortex (Xu et al., 2009). Finally, as ocular dominance shifts in visual cortex due to brief monocular deprivation, rapid loss of spines is also witnessed in the same region (Yu et al., 2011).

Finally, spine dynamics not only respond to learning, but also predict it. Roberts *et al* found that the amount spine turnover in the zebra finch HVC, a forebrain region critical for song learning, immediately before commencement of song learning correlated with future learning (Roberts et al., 2010). Specifically, animals with higher levels of spine turnover performed better on measures of song learning. Taken together these results suggest that structural plasticity expressed as experience- and learning-dependent changes to dendritic spine dynamics is an important mechanism for the brain to incorporate and store information and to dynamically rewire itself following injury.

1.4 Studies of Clustered Structural Plasticity

Results from studies of structural plasticity of dendrites have provided a number of pieces of evidence in support of clustered plasticity. To begin, Engert and Bonhoeffer utilized chronic two-photon microscopy in conjunction with a local glutamate superfusion system to track subcellular changes on dye-filled CA1 pyramidal neurons (Engert and Bonhoeffer, 1999). The authors demonstrated the ability to induce L-LTP using localized glutamate superfusion and

also find a region specific increase in the number of dendritic spines. That is, the specific region of dendrite that undergoes LTP also shows a lasting (up to 12 hours) increase in the number of dendritic spines present. This result shows that addition of spines is a potential mechanism to increase synaptic efficacy and that this process occurs in a localized fashion.

Toni *et al* expanded on the studies of Engert and Bonhoeffer by utilizing electron microscopy to examine the ultrastructural changes associated with induction of LTP at CA1 synapses (Toni et al., 1999). To facilitate specificity of their studies, the authors utilized a potassium chromium-tris-oxalate precipitation protocol during osmium fixation of the tissue which generates a fine, electron-dense precipitate in dendrites and dendritic spines which had recently experienced an increase in calcium concentration. The authors induced LTP utilizing a theta-burst stimulation (TBS) protocol and then waited 30-120 minutes before utilizing a second round of TBS to cause another increase in calcium in the potentiated synapses and allow for precipitation labeling. The authors found a significant increase in the number of axonal boutons making contact with more than one spine specifically for activated spines. These multi-spine boutons occurred by 45 minutes post TBS, were maintained at an increased level at the longest time point examined (120 minutes) and were dependent on α-calcium/calmodulin-dependent protein kinase II (αCaMKII), as their appearance was blocked by application of the αCaMKII inhibitor KN93. Utilizing three-dimensional reconstruction, the authors found that a majority (66%) of multi-spine boutons resulted from two or more spines from the same dendrite contacting the same axonal bouton. This finding suggests that new spines were added to potentiated segments of dendrite and that these spines frequently contacted the same presynaptic partner, perhaps as a mechanism to further strengthen synaptic contact between two cells. This was the first example of clustered spine addition, where newly added spines were spatially clustered on a dendrite.

De Roo *et al* found similar results in organotypic slice culture (De Roo et al., 2008). Specifically, the authors induced LTP via either TBS or by a 20-60 minute bath application of

carbachol and subsequently tracked structural changes to biolisticly transfected neurons expressing enhanced-GFP (EGFP). The authors found an increase in the number of new spines added up to four days after LTP induction while also seeing a decrease in stability of existing spines. The authors were then able to track spine responses to test stimulus pulses by filling neurons with the calcium indicator Fluo-4. Dendritic spines that expressed calcium transients in response to test pulses were more stable than non-responsive spines and also preferentially had new spines added nearby. While the presynaptic partners of the responsive spines and the newly added spines were not probed, the results again suggested that one mechanism for a neuron to express plasticity is to add new spines near active, potentiated spines.

Two recent studies have moved from studying structural plasticity following LTP induction in hippocampal slices to examining learning-related alterations in dendrite morphology in intact animals. The first such study utilized the auditory localization system of the barn owl to tract changes to axo-dendritic contacts (McBride et al., 2008). To begin, auditory localization in the barn owl is similar to that in humans in that binaural cues in conjunction with visual input are utilized to localize sound. Individual neurons in the external nucleus of the inferior colliculus (ICX) receive monosynaptic input from axons originating in the lateral shell of the central nucleus of the inferior colliculus (ICCls) and integrate this information. This synaptic connection is a site of plasticity (Knudsen and Knudsen, 1985) and alterations to connectivity between these cells can occur when animals are exposed to chronic optical displacement of the visual fields (“prism-rearing”). The topographic organization of ICCls axonal projections is typically distributed into three primary zones, a minority of axons in a right space zone, the majority of axons in a normal zone, and a minority of axons in a left space zone. With visual displacement (19 degrees in the present study), rewiring shifts this distribution so that more axons are found in the right space zone, which becomes adapted as the normal zone (the reverse is true for the opposing hemisphere). This allows the authors to examine the extent and localization of axonal

arborization in the various zones of ICX after prism-rearing and make statements concerning how the system has been altered without requiring chronic *in vivo* imaging. To do so, following prism-rearing, animals are sacrificed and slices are taken from the inferior colliculus. An anterograde tracer is injected into ICCIs and allowed to fill the axons of these neurons while the slice is maintained in aCSF. The tissue is then fixed and further stained for αCaMKII to label the dendrites of the auditory responsive neurons in ICX before analysis of axo-dendritic contacts is made using high resolution confocal microscopy.

First, the authors confirm by electrophysiology in intact animals that prism-rearing shifts auditory tuning toward adaptive locations by recording throughout the rostro-caudal extent of ICX. Prism-reared juveniles have a significant shift in auditory response magnitude toward the adaptive zone of ICX and away from the normal and maladaptive zones relative to normally-raised juvenile owls. The authors then conduct a structural analysis of the fixed tissue and find that the mean distance between axo-dendritic contacts of ICCIs with ICX neurons (inter-contact distance, ICD) is smaller in the adaptive zone in prism-reared animals (5.1 ± 0.23 μm) than the normal zone and closely mirrors the mean contact distance in the normal zone of normally-reared owls (4.4 ± 0.24 μm). When examining the full distribution of ICDs, the authors find that prism-adapted animals have a left shift of this curve, representing smaller values in the adaptive zone, with nearly all ICDs less than 20 μm. These results were the first to show that learning related changes to axo-dendritic structure supported the clustered plasticity hypothesis by finding a clustering of new synaptic contacts. The authors postulated that addition of closely spaced contacts of less than 20 μm occurs with concomitant elimination of widely spaced contacts and drives prism-induced rewiring, which allows for synergistic interaction of these contacts to drive strong postsynaptic responses in the adaptive zone of ICX.

The second study to examine the impact of learning on structural plasticity made use of a well-characterized motor learning task and two-photon *in vivo* imaging to chronically track changes to dendritic spines in primary motor cortex (Fu et al., 2012). Specifically, the authors

trained mice to reach through a slot in a Plexiglas box, grab a seed, and pull it back into the cage. By utilizing Thy1-Yellow Fluorescent Protein (YFP) mice, which strongly express YFP in a subset of layer 5 cortical pyramidal cells, and two-photon imaging, the authors were able to repeatedly image the same dendrites across multiple days and thus track dendritic spine dynamics. Previous work from the same group showed that mice were able to improve their successful reach rate in this seed reaching task and that this learning was associated with a transient increase in the rate of spine addition on the apical dendrites of layer 5 pyramidal neurons in primary motor cortex (Xu et al., 2009). Strikingly, the authors found that new spines added while the animals are learning the seed reaching task (i.e. before they have reached a behavioral plateau) were preferentially added within 5 μm of each other. This is to say that two or more new spines were formed during learning and existed within a physical distance of 5 μm from each other on the dendrite. This result was the first to show the dynamics of spine addition and clustering *in vivo* while an animal learns, and corroborated the findings from *ex vivo* slice work.

Excitingly, there are a number of unique properties of clustered spines that further suggest their importance for motor learning. First, spine head size, a well validated surrogate for synapse strength (Govindarajan et al., 2011; Carlisle and Kennedy, 2005), was found to increase during learning specifically for new spines added in clusters. This suggests that as spines are added in clusters, the synapses they contain are also potentiated. Further, newly added spines that appeared in clusters were more stable than newly added spines that appeared alone. Specifically, the authors re-imaged animals either two weeks or several months after motor learning and assessed the presence or absence of spines added during learning. In both cases, spines added in clusters preferentially survived to the remote imaging point when compared to new lone spines. Finally, spine clustering due to learning appears to be a task specific phenomenon. Specifically, in a separate set of experiments the authors began by training animals on the standard seed reaching task and then switch to training on a

pasta handling task which was also known to induce motor learning and spine addition. Animals undergoing the seed reaching alone task and animals undergoing the seed reaching coupled with pasta handling task had an increase in clustered spine formation. However, in cross trained animals (seed reaching followed by pasta handling), new spines added during seed reaching did not cluster with new spines added during pasta handling. This suggests that clustered spine addition is a task-specific property of motor learning.

Finally, evidence suggests that inhibitory and excitatory synapse dynamics are also spatially clustered. Chen *et al* utilized chronic *in vivo* two-photon imaging to track dendritic spine dynamics on layer 2/3 neurons in mouse visual cortex (Chen et al., 2012). Additionally, inhibitory synapses were identified and tracked over time by co-expression of a Teal-Gephyrin construct. The authors found not only that inhibitory synapses responded strongly to monocular deprivation with increased turnover rates, but also that gain and loss of inhibitory synapses preferentially occurred within 10 μm of gain and loss of both other inhibitory synapses and also excitatory synapses. Taken together, these results suggest that clustered structural plasticity occurs not only for excitatory synapses on dendritic spines, but also inhibitory synapses onto excitatory neurons. Further, the spatial proximity of excitatory and inhibitory synapse dynamics to each other suggests a coordination of these events, perhaps due to shared molecular cross talk.

1.5 Computational Studies of Clustered Plasticity

A wealth of data from biochemical studies of LTP, to electrophysiological studies of dendritic spikes and stimulus input, to structural studies of dendritic spines all find convergent evidence in support of the clustered plasticity hypothesis. However, why the nervous system appears to organize information storage in this way is still an open question. The non-linear properties of dendrites and their ability to integrate synaptic inputs locally are suggested as

potential reasons for clustered plasticity. *In silico* models of neuronal networks have probed this question and found exciting results that suggest clustered plasticity provides vastly increased storage capacity (Poirazi and Mel, 2001). Specifically, the authors used a biophysically detailed model neuron containing AMPA and NMDA-type synaptic conductances as well as low concentrations of voltage-dependent Na^+ and K^+ channels. Each model neuron contained *m* dendritic branches with *k* synapses per branch. To explore the effect of clustered inputs, the authors contrasted: 1) linear integration (i.e. the standard model) where the cell's activation level was calculated as a weighted sum of inputs spanning the entire cell, 2)non-linear integration where first the *k* synaptic inputs on each branch are combined in a weighted sum, a nonlinearity (such as a sigmoid or power function) is applied to each branch, and finally the nonlinear branch responses are summed to calculate the neuron's overall activation. Importantly, linear and nonlinear neurons differed only in their mode of integration, not in the numbers of branches or synapses present. Finally, neuronal responses were binary in this study, where firing of a cell indicated a positive response while lack of firing indicated a negative response.

With linear and nonlinear model neurons established, the authors were interested in assessing learning capacity. To do so, each neuron was "taught" to recognize and respond correctly to patterns of synaptic input that served as a training set and contain both positive and negative exemplars (i.e. the neuron should fire to certain patterns and not fire to other patterns). This learning process could be accomplished by changing the weights of pre-existing synapses or by eliminating a synapse and replacing it with a new contact. The objective was for the neuron to respond selectively to positive training exemplars and to have a uniform lack of response to negative exemplars. Memory capacity of each neuron was assessed in two ways: 1) analytically by deriving combinatorial expressions that count the number of unique input-output functions a neuron could produce by altering all possible settings of modifiable parameters (i.e. altering the ways in which synapses can be restructured to produce distinct receptive fields), 2) empirically by measuring how large a training set each neuron could learn

with a 2% error rate. Analytical analysis found that capacity of the nonlinear neuron increased nearly linearly with increases in number of branches, number of synapses per branch, and total neuron size. In fact, capacity for the nonlinear model was maximal for a neuron having 1250 branches with eight synapses each. Importantly, the analytical assessment of memory capacity closely matched the empiric measurement of pattern recognition for both linear and nonlinear models. Strikingly, empiric assessment revealed that a nonlinear neuron with 10,000 synapses learned 27,000 unique input patterns with an error rate of 2% while the linear model could accommodate only 600 patterns at the same 2% error rate; this was an increase in capacity by a factor of 46.

1.6 Goals of the Dissertation

To summarize, biochemical, electrophysiological, and structural studies find convergent evidence that plasticity within a neuron is not randomly distributed, but rather clustered into functional groups (Figure 1.2). *In vivo* structural studies of adaptation to sensory alteration and motor learning demonstrate that naturalistic experience is able to drive the formation of clusters of dendritic spines. Computational analysis suggests that clustering of plasticity allows for an increase in information storage capacity. However, it is unknown how pervasive structural clustering is and whether multiple forms of learning and memory also utilize dendritic spine clustering for information storage.

This thesis explores the prevalence and properties of clustered structural plasticity in mouse cortex. In Chapter 2 I evaluate structural plasticity by utilizing chronic *in vivo* two-photon imaging to track the gain, loss, and stability of spines on the apical dendrites of layer 5 pyramidal neurons in mouse retrosplenial cortex (RSC), both at baseline and during contextual fear conditioning. The retrosplenial cortex is a brain region critically involved in spatial learning and memory and is both activated by and required for contextual fear conditioning. I find that

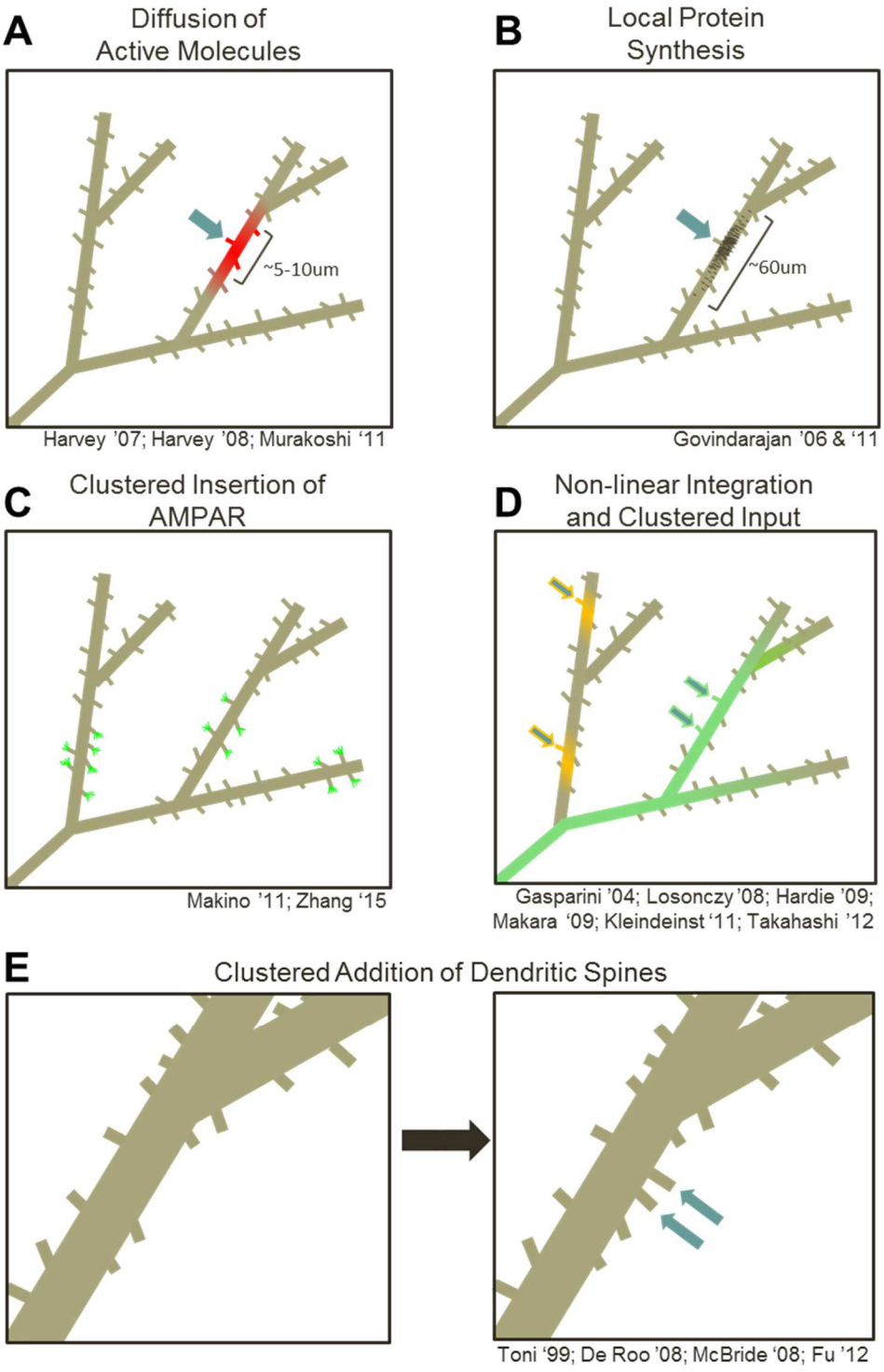

Figure 1.2: Summary of the clustered plasticity hypothesis.
Convergent evidence from various fields of neuroscience finds support for the clustered plasticity hypothesis. (A) Diffusion of activated molecules (H-ras/Rho-A) out of stimulated spines and into nearby spines within 5-10 um lowers the threshold for LTP induction. (B) Synaptic tag setting and capture of locally synthesized proteins facilitates LTP induction between spines over distances of tens of microns. (C) Clustered insertion of GluRI subunits of AMPARs in spines that are closely spaced demonstrates localized and clustered plasticity. (D) Non-linear electrical properties of dendrites allows for spatial and temporal integration of inputs, dendritic spike generation, and branch strength potentiation. (E) Addition of new dendritic spines near each other occurs during LTP and learning.

spatial learning due to contextual fear conditioning increases the proportion of new spines that form in clusters within 5 μm of each other specifically in retrosplenial cortex. Additionally, clustered spine addition correlates with behavioral performance in the contextual fear conditioning paradigm. In Chapter 3 I evaluate the spatial distribution of spine changes in RSC and find that spine loss occurs at a reduced spatial frequency and preferentially near clustered new spines following spatial learning. In Chapter 4 I examine the hypothesis that spine turnover before learning correlates with future learning. I find that spine turnover in RSC in the days before training commences correlates with future learning. Together, these results suggest that dynamic control of both clustered addition and loss of dendritic spines is a mechanism for information storage in retrosplenial cortex. Finally, in Chapter 5 I integrate the results from the previous chapters and suggest future experiments to further the study of clustered plasticity in mouse RSC.

1.7 References

Arellano, J. I., Espinosa, A., Fairén, A., Yuste, R., & DeFelipe, J. (2007). Non-synaptic dendritic spines in neocortex. *Neuroscience*, *145*, 464–469.

Ballesteros-Yanez, I., Benavides-Piccione, R., Elston, G. N., Yuste, R., & DeFelipe, J. (2006). Density and morphology of dendritic spines in mouse neocortex. *Neuroscience*, *138*(2), 403–409.

Beaulieu, C., & Colonnier, M. (1987). Effect of the richness of the environment on the cat visual cortex. *The Journal of Comparative Neurology*, *266*, 478–494.

Carlisle, H. J., & Kennedy, M. B. (2005). Spine architecture and synaptic plasticity. *Trends in Neurosciences*, *28*(4), 182–187.

Chen, J. L., Villa, K. L., Cha, J. W., So, P. T. C., Kubota, Y., & Nedivi, E. (2012). Clustered Dynamics of Inhibitory Synapses and Dendritic Spines in the Adult Neocortex. *Neuron*, *74*(2), 361–373.

Chen, X., Leischner, U., Rochefort, N. L., Nelken, I., & Konnerth, A. (2011). Functional mapping of single spines in cortical neurons in vivo. *Nature*, *475*(7357), 501–505.

Chow, D. K., Groszer, M., Pribadi, M., Machniki, M., Carmichael, S. T., Liu, X., & Trachtenberg, J. T. (2009). Laminar and compartmental regulation of dendritic growth in mature cortex. *Nature Neuroscience*, *12*(2), 116–118.

Colonnier, M. (1968). Synaptic patterns on different cell types in the different laminae of the cat visual cortex. An electron microscope study. *Brain Research*, *9*, 268–287.

De Felipe, J., Marco, P., Fairén, A., & Jones, E. G. (1997). Inhibitory synaptogenesis in mouse somatosensory cortex. *Cerebral Cortex*, *7*, 619–634.

De Roo, M., Klauser, P., & Muller, D. (2008). LTP promotes a selective long-term stabilization and clustering of dendritic spines. *PLoS Biology*, *6*(9), e219.

Engert, F., & Bonhoeffer, T. (1999). Dendritic spine changes associated with hippocampal long-term synaptic plasticity. *Nature*, *399*(6731), 66–70.

Fiala, J. C., Feinberg, M., Popov, V., & Harris, K. M. (1998). Synaptogenesis via dendritic filopodia in developing hippocampal area CA1. *The Journal of Neuroscience : The Official Journal of the Society for Neuroscience*, *18*(21), 8900–8911.

Fu, M., Yu, X., Lu, J., & Zuo, Y. (2012). Repetitive motor learning induces coordinated formation of clustered dendritic spines in vivo. *Nature*, *483*(7387), 92–5.

Gasparini, S., Migliore, M., & Magee, J. C. (2004). On the initiation and propagation of dendritic spikes in CA1 pyramidal neurons. *The Journal of Neuroscience : The Official Journal of the Society for Neuroscience*, *24*(49), 11046–56.

Geinisman, Y., Berry, R. W., Disterhoft, J. F., Power, J. M., & Van der Zee, E. A. (2001). Associative learning elicits the formation of multiple-synapse boutons. *The Journal of Neuroscience : The Official Journal of the Society for Neuroscience*, *21*(15), 5568–73.

Govindarajan, A., Israely, I., Huang, S.-Y., & Tonegawa, S. (2011). The Dendritic Branch Is the Preferred Integrative Unit for Protein Synthesis-Dependent LTP. *Neuron*, *69*(1), 132–146.

Govindarajan, A., Kelleher, R. J., & Tonegawa, S. (2006). A clustered plasticity model of long-term memory engrams. *Nature Reviews. Neuroscience*, *7*(7), 575–83.

Greenough, W. T., Hwang, H. M., & Gorman, C. (1985). Evidence for active synapse formation or altered postsynaptic metabolism in visual cortex of rats reared in complex environments. *Proceedings of the National Academy of Sciences of the United States of America*, *82*, 4549–4552.

Grutzendler, J., Kasthuri, N., & Gan, W.-B. (2002). Long-term dendritic spine stability in the adult cortex. *Nature*, *420*(6917), 812–6.

Hardie, J., & Spruston, N. (2009). Synaptic depolarization is more effective than back-propagating action potentials during induction of associative long-term potentiation in

hippocampal pyramidal neurons. *The Journal of Neuroscience : The Official Journal of the Society for Neuroscience*, *29*(10), 3233–41.

Harris, K. M., Jensen, F. E., & Tsao, B. (1992). Three-dimensional structure of dendritic spines and synapses in rat hippocampus (CA1) at postnatal day 15 and adult ages: implications for the maturation of synaptic physiology and long-term potentiation. *The Journal of Neuroscience : The Official Journal of the Society for Neuroscience*, *12*(July), 2685–2705.

Harris, K. M., & Kater, S. B. (1994). Dendritic spines: cellular specializations imparting both stability and flexibility to synaptic function. *Annual Review of Neuroscience*, *17*, 341–371.

Harris, K. M., & Stevens, J. K. (1989). Dendritic spines of CA 1 pyramidal cells in the rat hippocampus: serial electron microscopy with reference to their biophysical characteristics. *The Journal of Neuroscience : The Official Journal of the Society for Neuroscience*, *9*, 2982–2997.

Harvey, C. D., & Svoboda, K. (2007). Locally dynamic synaptic learning rules in pyramidal neuron dendrites. *Nature*, *450*(7173), 1195–200.

Harvey, C. D., Yasuda, R., Zhong, H., & Svoboda, K. (2008). The spread of Ras activity triggered by activation of a single dendritic spine. *Science (New York, N.Y.)*, *321*(5885), 136–40.

Hofer, S. B., Mrsic-Flogel, T. D., Bonhoeffer, T., & Hübener, M. (2009). Experience leaves a lasting structural trace in cortical circuits. *Nature*, *457*(7227), 313–7.

Holtmaat, A. J. G. D., Trachtenberg, J. T., Wilbrecht, L., Shepherd, G. M., Zhang, X., Knott, G. W., & Svoboda, K. (2005). Transient and persistent dendritic spines in the neocortex in vivo. *Neuron*, *45*(2), 279–91.

Holtmaat, A., Wilbrecht, L., Knott, G. W., Welker, E., & Svoboda, K. (2006). Experience-dependent and cell-type-specific spine growth in the neocortex. *Nature*, *441*(7096), 979–83.

Holtmaat, A., & Svoboda, K. (2009). Experience-dependent structural synaptic plasticity in the mammalian brain. *Nature Reviews. Neuroscience*, *10*(9), 647–58.

Jia, H., Rochefort, N. L., Chen, X., & Konnerth, A. (2010). Dendritic organization of sensory input to cortical neurons in vivo. *Nature*, *464*(7293), 1307–12.

Jung, C. K. E., & Herms, J. (2012). Structural Dynamics of Dendritic Spines are Influenced by an Environmental Enrichment: An In Vivo Imaging Study. *Cerebral Cortex (New York, N.Y. : 1991)*, *24*, 377–384.

Keck, T., Mrsic-Flogel, T. D., Vaz Afonso, M., Eysel, U. T., Bonhoeffer, T., & Hübener, M. (2008). Massive restructuring of neuronal circuits during functional reorganization of adult visual cortex. *Nature Neuroscience*, *11*(10), 1162–7.

Kleindienst, T., Winnubst, J., Roth-Alpermann, C., Bonhoeffer, T., & Lohmann, C. (2011). Activity-dependent clustering of functional synaptic inputs on developing hippocampal dendrites. *Neuron*, *72*(6), 1012–24.

Knott, G. W., Holtmaat, A., Wilbrecht, L., Welker, E., & Svoboda, K. (2006). Spine growth precedes synapse formation in the adult neocortex in vivo. *Nature Neuroscience*, *9*(9), 1117–24.

Knott, G. W., Quairiaux, C., Genoud, C., & Welker, E. (2002). Formation of dendritic spines with GABAergic synapses induced by whisker stimulation in adult mice. *Neuron*, *34*, 265–273.

Knudsen, E. I., & Knudsen, P. F. (1985). Vision guides the adjustment of auditory localization in young barn owls. *Science (New York, N.Y.)*, *230*, 545–548.

Kolb, B., Cioe, J., & Comeau, W. (2008). Contrasting effects of motor and visual spatial learning tasks on dendritic arborization and spine density in rats. *Neurobiology of Learning and Memory*, *90*, 295–300.

Lai, C. S. W., Franke, T. F., & Gan, W.-B. (2012). Opposite effects of fear conditioning and extinction on dendritic spine remodeling. *Nature*, *483*(7387), 87–91.

Larkum, M. E., & Nevian, T. (2008). Synaptic clustering by dendritic signaling mechanisms. *Current Opinion in Neurobiology*, *18*(3), 321–31.

Lee, W. C. A., Huang, H., Feng, G., Sanes, J. R., Brown, E. N., So, P. T., & Nedivi, E. (2006). Dynamic remodeling of dendritic arbors in GABAergic interneurons of adult visual cortex. *PLoS Biology*, *4*, 271–280.

Lendvai, B., Stern, E. A., Chen, B., & Svoboda, K. (2000). Experience-dependent plasticity of dendritic spines in the developing rat barrel cortex in vivo. *Nature*, *404*(6780), 876–81.

Losonczy, A., Makara, J. K., & Magee, J. C. (2008). Compartmentalized dendritic plasticity and input feature storage in neurons. *Nature*, *452*(7186), 436–41.

Magee, J. C., & Johnston, D. (1997). A synaptically controlled, associative signal for Hebbian plasticity in hippocampal neurons. *Science (New York, N.Y.)*, *275*, 209–213.

Majewska, A. K., Newton, J. R., & Sur, M. (2006). Remodeling of synaptic structure in sensory cortical areas in vivo. *The Journal of Neuroscience : The Official Journal of the Society for Neuroscience*, *26*(11), 3021–3029.

Makara, J. K., Losonczy, A., Wen, Q., & Magee, J. C. (2009). Experience-dependent compartmentalized dendritic plasticity in rat hippocampal CA1 pyramidal neurons. *Nature Neuroscience*, *12*(12), 1485–1487.

Makino, H., & Malinow, R. (2011). Compartmentalized versus global synaptic plasticity on dendrites controlled by experience. *Neuron*, *72*(6), 1001–11.

McBride, T. J., Rodriguez-Contreras, A., Trinh, A., Bailey, R., & Debello, W. M. (2008). Learning drives differential clustering of axo-dendritic contacts in the barn owl auditory system. *The Journal of Neuroscience : The Official Journal of the Society for Neuroscience*, *28*(27), 6960–73.

McGuire, B. a, Hornung, J. P., Gilbert, C. D., & Wiesel, T. N. (1984). Patterns of synaptic input to layer 4 of cat striate cortex. *The Journal of Neuroscience*, *4*, 3021–33.

Micheva, K. D., & Smith, S. J. (2007). Array Tomography: A New Tool for Imaging the Molecular Architecture and Ultrastructure of Neural Circuits. *Neuron*, *55*, 25–36.

Miller, S., & Mayford, M. (1999). Cellular and molecular mechanisms of memory: The LTP connection. *Current Opinion in Genetics and Development*.

Mizrahi, A., & Katz, L. C. (2003). Dendritic stability in the adult olfactory bulb. *Nature Neuroscience*, *6*, 1201–1207.

Moczulska, K. E., Tinter-Thiede, J., Peter, M., Ushakova, L., Wernle, T., Bathellier, B., & Rumpel, S. (2013). Dynamics of dendritic spines in the mouse auditory cortex during memory formation and memory recall. *Proceedings of the National Academy of Sciences of the United States of America*, *110*(45), 18315–20.

Moser, M. B., Trommald, M., & Andersen, P. (1994). An increase in dendritic spine density on hippocampal CA1 pyramidal cells following spatial learning in adult rats suggests the formation of new synapses. *Proceedings of the National Academy of Sciences of the United States of America*, *91*(December), 12673–12675.

Murakoshi, H., Wang, H., & Yasuda, R. (2011). Local, persistent activation of Rho GTPases during plasticity of single dendritic spines. *Nature*, *472*(7341), 100–4.

Nägerl, U. V., Köstinger, G., Anderson, J. C., Martin, K. C., & Bonhoeffer, T. (2007). Protracted synaptogenesis after activity-dependent spinogenesis in hippocampal neurons. *The Journal of Neuroscience : The Official Journal of the Society for Neuroscience*, *27*(30), 8149–56.

Peters, A., & Kaiserman-Abramof, I. R. (1970). The small pyramidal neuron of the rat cerebral cortex. The perikaryon, dendrites and spines. *The American Journal of Anatomy*, *127*, 321–355.

Poirazi, P., & Mel, B. W. (2001). Impact of active dendrites and structural plasticity on the memory capacity of neural tissue. *Neuron*, *29*(3), 779–96.

Rakic, P., Bourgeois, J. P., Eckenhoff, M. F., Zecevic, N., & Goldman-Rakic, P. S. (1986). Concurrent overproduction of synapses in diverse regions of the primate cerebral cortex. *Science (New York, N.Y.)*, *232*, 232–235.

Remy, S., & Spruston, N. (2007). Dendritic spikes induce single-burst long-term potentiation. *Proceedings of the National Academy of Sciences of the United States of America*, *104*, 17192–17197.

Roberts, T. F., Tschida, K. A., Klein, M. E., & Mooney, R. (2010). Rapid spine stabilization and synaptic enhancement at the onset of behavioural learning. *Nature*, *463*(7283), 948–52.

Schallert, T., Leasure, J. L., & Kolb, B. (2000). Experience-associated structural events, subependymal cellular proliferative activity, and functional recovery after injury to the central nervous system. *Journal of Cerebral Blood Flow and Metabolism : Official Journal of the International Society of Cerebral Blood Flow and Metabolism*, *20*, 1513–1528.

Shepherd, G. M., & Harris, K. M. (1998). Three-dimensional structure and composition of CA3-->CA1 axons in rat hippocampal slices: implications for presynaptic connectivity and compartmentalization. *The Journal of Neuroscience : The Official Journal of the Society for Neuroscience*, *18*(20), 8300–8310.

Spacek, J. (1982). “Free” postsynaptic-like densities in normal adult brain: their occurrence, distribution, structure and association with subsurface cisterns. *Journal of Neurocytology*, *11*, 693–706.

Spruston, N. (2008). Pyramidal neurons: dendritic structure and synaptic integration. *Nature Reviews. Neuroscience*, *9*(3), 206–21.

Takahashi, N., Kitamura, K., Matsuo, N., Mayford, M., Kano, M., Matsuki, N., & Ikegaya, Y. (2012). Locally Synchronized Synaptic Inputs. *Science*, *335*(6066), 353–356.

Toni, N., Buchs, P., Nikonenko, I., & Bron, C. (1999). LTP promotes formation of multiple spine synapses between a single axon terminal and a dendrite. *Nature*, *402*(November), 421–425.

Toni, N., Teng, E. M., Bushong, E. a, Aimone, J. B., Zhao, C., Consiglio, A., … Gage, F. H. (2007). Synapse formation on neurons born in the adult hippocampus. *Nature Neuroscience*, *10*(6), 727–734.

Trachtenberg, J. T., Chen, B. E., Knott, G. W., Feng, G. P., Sanes, J. R., Welker, E., & Svoboda, K. (2002). Long-term in vivo imaging of experience-dependent synaptic plasticity in adult cortex. *Nature*, *420*(6917), 788–794.

Varga, Z., Jia, H., Sakmann, B., & Konnerth, A. (2011). Dendritic coding of multiple sensory inputs in single cortical neurons in vivo. *Proceedings of the National Academy of Sciences of the United States of America*, *108*(37), 15420–5.

Xu, T., Yu, X., Perlik, A. J., Tobin, W. F., Zweig, J. a, Tennant, K., … Zuo, Y. (2009). Rapid formation and selective stabilization of synapses for enduring motor memories. *Nature*, *462*(7275), 915–9.

Yu, H., Majewska, A. K., & Sur, M. (2011). Rapid experience-dependent plasticity of synapse function and structure in ferret visual cortex in vivo. *Proceedings of the National Academy of Sciences*, *108*(52), 21235–21240.

Zhang, Y., Cudmore, R. H., Lin, D.-T., Linden, D. J., & Huganir, R. L. (2015). Visualization of NMDA receptor–dependent AMPA receptor synaptic plasticity in vivo. *Nature Neuroscience*, *18*(3).

Zito, K., Parnas, D., Fetter, R. D., Isacoff, E. Y., & Goodman, C. S. (1999). Watching a synapse grow: Noninvasive confocal imaging of synaptic growth in Drosophila. *Neuron*, *22*, 719–729.

Zito, K., Scheuss, V., Knott, G., Hill, T., & Svoboda, K. (2009). Rapid Functional Maturation of Nascent Dendritic Spines. *Neuron*, *61*(2), 247–258.

Zuo, Y., Lin, A., Chang, P., & Gan, W.-B. (2005a). Development of long-term dendritic spine stability in diverse regions of cerebral cortex. *Neuron*, *46*(2), 181–9.

Zuo, Y., Yang, G., Kwon, E., & Gan, W.-B. (2005b). Long-term sensory deprivation prevents dendritic spine loss in primary somatosensory cortex. *Nature*, *436*(July), 261–265.

Chapter 2

Spatial Learning Induces Clustered Spine Formation in Retrosplenial Cortex

2.1 Introduction

2.1.1 Retrosplenial Cortex

The retrosplenial cortex (RSC) is a midline cortical structure that extends over half the length of the cerebrum (from -0.94 to -4.48 millimeters (mm) anterior/posterior of Bregma in the mouse) and is one of the largest cortical structures in the rodent brain (Vogt and Paxinos, 2012; Vann et al., 2009). The RSC is broadly divided into three regions based on cytoarchitecture and connectivity: the dysgranular region, the granular A region, and the granular B region (Van Groen and Wyss, 1990; Van Groen and Wyss, 1992; Van Groen et al., 2003). Further, RSC is considered an intermediate cortex as standard cortical laminations are not present throughout. Rather, lamination increases in a lateral to medial direction and reaches six layers in the dysgranular region, though with a poorly defined dysgranular layer 4 (Vann et al., 2009). The RSC is a highly interconnected cortical region. Specifically, the rodent RSC is densely and reciprocally connected with the anterior thalamic nuclei, the lateral dorsal thalamic nuclei, and the hippocampal formation (postsubiculum, subiculum, and presubiculum), regions that, based solely on connectivity, would suggest a role for RSC in learning and memory. Further, the RSC is reciprocally connected to the anterior cingulate cortex (Van Groen and Wyss, 1992; Jones et

al., 2005) and Broadmann areas 46 and 9 of the dorsolateral prefrontal cortex (Morris et al., 1999). The RSC receives visual information via direct inputs from V2 and V4 (Vogt, 1985) and through connections with Broadmann areas 18b and 17 (Vogt and Mill, 1983) and has subcortical inputs from the raphe nuclei, the locus coeruleus, and the diagonal band (Vogt, 1985).

As mentioned, connectivity of the RSC alone would suggest a role in learning and memory, though a multitude of animal and human studies support this conjecture. Classic studies of RSC function relied on electrolytic, excitotoxic, and aspiration lesions, which, while often varying in extent and location, revealed a role for RSC in spatial memory and navigation. Specifically, lesions of RSC are shown to impair performance in the Morris water maze (Vann and Aggleton, 2002; Sutherland et al., 1988; Harker et al., 2004; Whishaw et al., 2001, Vann et al., 2003), the radial-arm maze (Vann and Aggleton, 2002, St-Laurent et al., 2009), object-place recognition (Vann and Aggleton, 2002), contextual fear conditioning (Keene and Bucci, 2008), and active avoidance in a two-way shuttle box (Lukoyanov et al., 2006).

Electrophysiological studies of RSC are consistent with its role in spatial learning and navigation. Specifically, approximately 10% of RSC neurons, equally distributed between dysgranular and granular RSC, are head-direction cells, which increase firing rates when an animal's head is in a preferred direction (Chen et al., 1994). Furthermore, while place cells have not been found in RSC, cells that modulate their firing based on combinations of location, movement, direction, and reward location have been identified (Cho and Sharp, 2001; Tabuchi et al., 2005; Smith et al., 2011). Electrophysiological studies of RSC have also confirmed its functional connections to anterior thalamus and the hippocampal formation. Specifically, lesions of dysgranular RSC disrupt head directions cells in anterior dorsal thalamic nuclei, causing a loss in stability in preferred firing direction (Taube, 2007); and, temporary inactivation of RSC with tetracaine causes a transient alteration to the spatial tuning of hippocampal place cells (Cooper and Mizumori, 2001).

Studies of immediate early gene (IEG) expression have also confirmed a role for RSC in learning and memory. Specifically, c-fos expression was increased in animals following radial arm maze exploration when familiar spatial cues were utilized for navigation (Vann et al., 2000; Amin et al., 2006) as well as when cues were removed (i.e. exploration in the dark) (Pothuizen et al., 2009). Contextual fear conditioning also induced IEG expression: c-fos was induced in RSC in animals exposed to a novel context and in animals contextually fear conditioned in this context (Robinson et al., 2012). Arc expression, however, was selectively increased in animals undergoing contextual fear conditioning (Robinson et al., 2012). Interestingly, in this same study, the authors found a functional link between RSC and the postrhinal cortex (POR) by utilizing retrograde tracer injected into POR to label RSC neurons projecting to this region. They found that following fear conditioning, approximately 30% of RSC neurons projecting to POR were c-fos positive, significantly more than the 5% positive in the home cage control animals. Finally, if RSC and POR were lesioned on contralateral sides (i.e. right RSC and left POR) giving a complete disconnection of the two structures in both hemispheres, freezing was significantly reduced in a 24-hour context recall test (Robinson et al., 2012).

Two recent inactivation studies confirmed a role for RSC in contextual fear conditioning (Corcoran et al., 2011) and Morris water maze (Czajkowski et al., 2014) and suggested cellular mechanisms operating within this structure that subserve its function in spatial memory. Specifically, Corcoran *et al* utilized infusions of APV directly into RSC to block activation of NMDARs. Strikingly, the authors found that NMDAR activity in RSC was not required during acquisition of contextual fear, but was required for fear recall at both recent (2 days post-training) and remote (36 days post-training) time points, suggesting that RSC may be a unique cortical structure in being required not just for remote but also for recent memory (Frankland and Bontempi, 2005). Surprisingly, Corcoran *et al* did not find a significant deficit in fear memory retrieval at recent or remote time points (2 days or 36 days post-training) when AMPAR activity was blocked by infusion of CNQX. This is in contrast to Czajkowski *et al* who found

deficits in Morris water maze performance due to RSC inactivation with CNQX. Specifically, animals were trained for 7 days and then split into two groups, a saline control group and a CNQX experimental group. Twenty-four hours after the final training day both groups were given a probe trial (an "Atlantis" platform was utilized to prevent extinction) without infusion and found to have equivalent learning and recall on all measures tested (target quadrant occupancy, platform crossings, average speed, time in zone (10, 15, and 20 centimeters (cm) around platform), and target proximity (measured for 15, 30, and 60 seconds)). Twenty-four hours later, animals were infused with either saline or CNQX and given a second probe trial: CNQX infused animals had a significant decrease in platform crossings and time in target zone (10 cm) and an increase in target proximity (15 sec), suggesting AMPAR function is necessary for memory recall in Morris water maze. More striking were the novel findings from this study obtained by utilizing two-photon *in vivo* imaging in c-fos-GFP transgenic animals to chronically track c-fos expression. The authors found that a significant portion of cells in RSC were reactivated (i.e. expressed c-fos) when trained in water maze to search for a platform in a similar location, suggesting a role for these cells in memory of the platform location. Strikingly, the authors found an enhancement in water maze probe trial performance (target quadrant occupancy, platform crossings, and 60 sec target proximity) when animals were infused with an HSV-CREB-Allatostatin receptor virus. Further, inactivation of the infected cells by infusion of allatostatin abolished this enhancement. This procedure of CREB virus infusion has previously been shown to recruit memory to CREB infected cells (Silva et al., 2009; Zhou et al., 2009; Han et al., 2009), suggesting that RSC is involved in memory storage and that CREB activity is able to recruit memory to specific cells.

Finally, direct activation of RSC has demonstrated its role in spatial learning and memory (Cowansage et al., 2014). Cowansage *et al* utilized a double transgenic system to tag, and subsequently re-activate, neurons activated specifically during contextual fear conditioning. Specifically, the Tet Tag mouse line (Reijmers et al., 2007), which expresses the tetracycline-

sensitive transactivator (tTA) under the control of the c-fos promoter, was crossed with a tetO-ChEF-tdTomato transgenic line. Double transgenic animals allowed for expression of the chanelrhodopsin variant, ChEF, in active neurons selectively when animals were not administered doxycycline (Dox), a tetracycline derivative that inhibits tTA binding to the tetO promoter. The authors selectively tagged neurons activated by contextual fear conditioning by removing of Dox-chow several days in advance of training (to allow for clearance of Dox) and by immediately placing animals back on Dox-chow following training. Expression of ChEF in RSC significantly increased in animals undergoing contextual fear conditioning relative to home cage controls. The authors confirmed the functionality of ChEF via whole cell recording in acute slices and by demonstrating an increase in c-fos expression in RSC following activation of ChEF via blue LED through a cranial window. Strikingly, the authors found that both unilateral and bilateral LED stimulation of ChEF expressing neurons in RSC twenty-four hours after training was able to induce freezing behavior in a novel context. Further, freezing stimulated by light exposure was correlated with post-shock freezing during training, was context specific - as tagging neurons in a different context from training caused no increase in freezing do to LED exposure – and engaged similar neuronal populations as natural recall (basal amygdala, central nucleus of the amygdala, and entorhinal cortex). Finally, inactivation of the hippocampus via CNQX/TTX blocked fear memory retrieval, but did not inhibit freezing due to LED activation of RSC. Taken together, these results demonstrate a role for RSC in recent contextual fear memory storage and retrieval and suggest a role dissociable from the hippocampus.

2.1.2 Rationale

Convergent data from biochemical, electrophysiological, and computational studies find evidence for clustered plasticity. Recently, structural studies of axo-dendritic contacts in barn owl auditory processing nuclei demonstrated that adaptation to changes in sensory input can cause clustering of putative synaptic contacts between cells involved in sensory processing

(McBride et al., 2008). Additionally, chronic *in vivo* imaging has shown that motor learning drives clustered addition of dendritic spines in mouse primary motor cortex (Fu et al., 2012). However, it is currently unknown whether structural clustering - due to learning or sensory adaptation - is restricted to primary cortical areas or extends to multimodal cortices as well. Additionally, it is unknown if dendritic spine clustering is unique to non-declarative motor learning or if formation of episodic-like memories also induces clustered spine formation. To address these questions we utilized chronic *in vivo* two-photon imaging to assess dendritic spine dynamics in mouse retrosplenial cortex during episodic-like spatial learning.

2.2 Methods

Surgery and Cranial Window Implantation

All experiments were conducted in accordance with the guidelines established by the UCLA Animal Research Committee. Adult (3-6 months old), singly housed male and female Thy1-YFP-H mice were used for all experiments. Animals were kept on a 12:12-h light:dark cycle with food and water *ad libitum*. All experiments were conducted during animals' light cycle. Importantly, 4 separate replicates of behavior and imaging in RSC were run. The data from all 4 replicates were pooled. Results for motor cortex behavior and imaging were collected from a single experiment. The size of each replicate was chosen to include approximately equal numbers of trained and control mice and to maximize the number of animals able to be imaged in one replicate cycle (approximately 8-12 mice).

The procedure we utilized for window implantation has been described in detail (Holtmaat et al., 2009); briefly, mice were anesthetized with isoflurane, placed in a stereotaxic frame, and kept warm with a monitored heating pad. Custom cut coverslips (square, 2x2 mm) were cleaned in ethanol and sterilized. A square region of skull 2 mm in width was marked using stereotactic coordinates (RSC: center at bregma -2.5 mm A/P; primary motor cortex: +1.8 mm

A/P, -1.5 mm M/L). The skull was thinned with a dental drill and removed. After the surgical site was cleaned with saline, the coverslip was placed on the dural surface and fastened with adhesive and dental acrylics to expose a square window of approximately 2 mm. Next, an aluminum bar with a threaded hole was attached to stabilize the mice during imaging sessions. Finally, mice were maintained on antibiotics during recovery and also given daily injections of carprofen and dexamethasone for one week to reduce inflammation. Mice were allowed to recover for two weeks before the first imaging session.

Behavioral Paradigm

While animals were recovering from surgery they were also handled and habituated to transport cues for two weeks. On the first day after handling and habituation mice underwent the first home cage baseline imaging session (Figure 2.1A). Two days later mice underwent the second baseline imaging session. The following day half the mice were randomly selected to begin contextual fear conditioning using a multi-day paradigm.

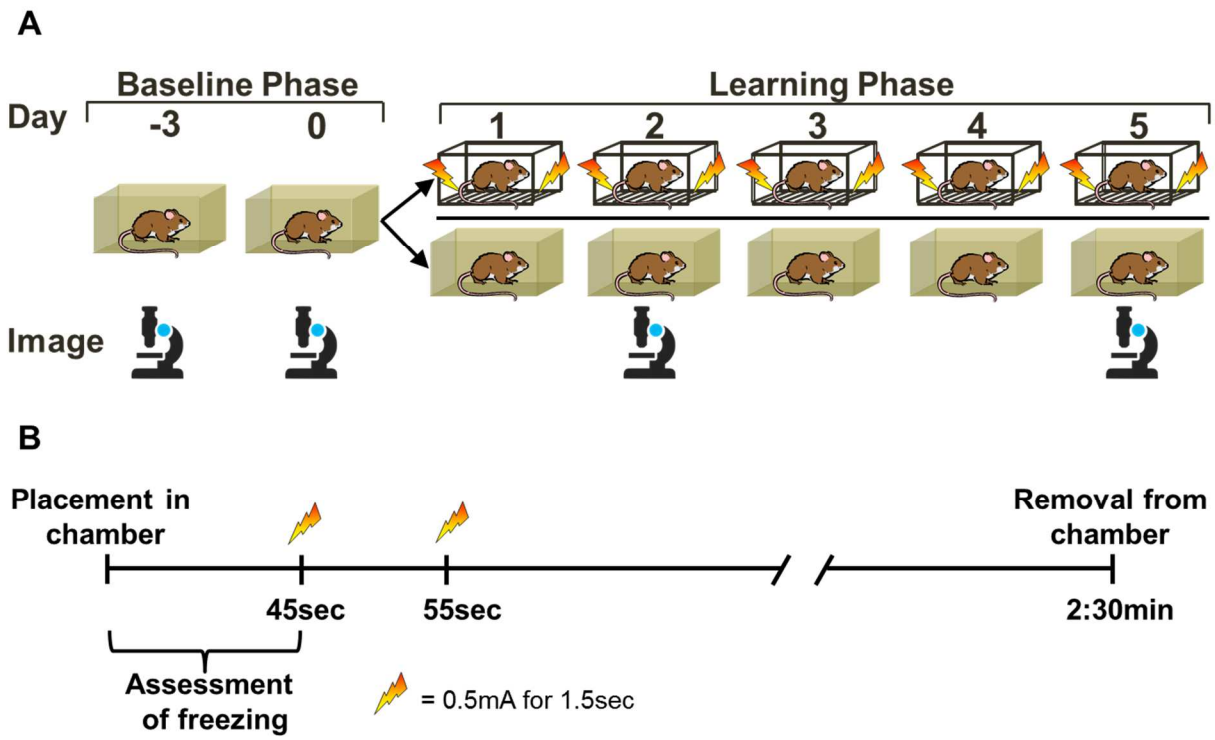

Figure 2.1: Behavioral protocol for contextual fear conditioning and two-photon imaging.
(A) Animals were imaged twice at baseline before contextual fear conditioning commenced (Day -3 and Day 0). Contextual fear conditioning began on Day 1. Animals were imaged again after conditioning on Day 2 and Day 5. (B) Animals were given 15 seconds prior to shock to explore the context. This time was also used to assess for freezing behavior. Two shocks were administered 10 seconds apart and animals were removed from the training chamber two minutes after the second shock.

Animals were placed in conditioning chambers, 45 seconds later were given one 1.5-second 0.5 milliamp shock, and 10 seconds later were given a second shock of the same intensity and duration (Figure 2.1B). Animals were removed from the conditioning chamber after a total of two minutes and 30 seconds in the chamber and placed in their home cage. On day 2 mice were conditioned again as on day 1, except that 90 minutes after conditioning mice were imaged. Training continued as above for a total of five days. Each conditioning chamber (32 cm wide, 25 cm high, 25 cm deep) was equipped with stainless steel grid floor (36 rods, each rod 2-mm diameter, 8-mm center to center; Med-Associates Inc., Georgia, VT) and stainless steel drop-pan. Chambers were scented with 100% isopropyl alcohol to provide a background odor. Each chamber was equipped with an overhead LED light source providing white light. Each chamber was connected to a solid-state scrambler, providing AC constant

current shock, controlled via an interface connected to a Windows computer running Video Freeze (Med-Associates Inc., Georgia, VT), a program designed for the automated assessment of freezing, an index of fear memory. Freezing was assessed in the 45 seconds prior to shock administration on each day of training. A second measure of fear memory, learning rate, was also utilized. Learning rate for each mouse was calculated as the slope of the line connecting baseline freezing on day 0 and the asymptote level of freezing on the day this occurred. The asymptote level of freezing was assessed as the highest freezing that occurred chronologically before any decrease in freezing occurred. Slope (m) was then calculated as m = (asymptote freezing – baseline freezing) / (day of asymptote freezing – day 0 of training).

Two-Photon Imaging

A custom-built laser scanning microscope was paired with a Spectra-Physics two-photon laser tuned to 920 nanometers (nm) and utilized for all imaging sessions. A 40x 1.0 numerical aperture (NA) water immersion objective (Zeiss) was used to acquire images at baseline and 90 minutes after each behavioral session. Mice were lightly anesthetized with isoflurane and attached to the head mount using a small screw and the aluminum bar which was fastened to the skull with dental acrylic. During the first imaging session on Baseline Imaging Day 1 (Day -3 of training), segments of apical dendrites from layer 5 pyramidal cells were imaged. The same segments were repeatedly imaged across experimental days by locating their position via a coordinate system established during the first imaging session.

Image Analysis

Dendritic spines were counted and analyzed by established criteria (Holtmaat et al., 2009). Specifically, the Spine Analysis software included in ScanImage was used to open all imaging days for a given segment of dendrite for a given animal. A segment is classified as the entire visible length of a branch of dendrite; and segments were often followed across several images. The presence, gain, and loss of spines were quantified across days for each segment,

and all segments were examined for a given animal. Importantly, all images were coded following completion of the experiment so that the experimenter was blind to training status of all mice while counting and analyzing spines. Additionally, if all segments of dendrite were not clearly imaged on each day of imaging, spines were not counted for this animal and it was not included in the analysis (n= 4 trained animals, n=2 control animals). Clustering of new spines was assessed following completion of counting of all spines for all animals in a given replicate. For each animal, the distance between new spines added during learning (Imaging Day 2 and Day 5) on the same segment of dendrite was calculated using the distance measurement tool in the Spine Analysis software. Spines within 5 μm of each other were counted as clustered. The percentage of clustered spines for each animal was calculated as the number of new spines within 5 μm of each other added during learning (added on Imaging Day 2 and persistent to Imaging Day 5 or added on Imaging Day 5) divided by the total number of spines added during learning.

Statistics

All group comparisons were calculated using Mann-Whitney U test to account for the non-normality of the data. Similarly, all correlations were calculated as Spearman's rho. All p-values represent results from two-sided tests, $\alpha=0.05$.

For the permutation test of clustering, all spines (whether gained, lost, or stable) from baseline imaging 2 to learning day 5 were analyzed for each segment of dendrite and the results aggregated across all animals. For each permutation, the number of new spines present on a given segment was assessed and this number was utilized to permute spine type (e.g., if three new spines were added to a segment of dendrite and the segment contained 15 total spines, for each permutation three random spines of the 15 total would be considered new and analyzed for clustering). The percentage of these selected spines within 5 μm of each other was calculated. This process was repeated 100,000 times and the resulting percentages

compared to the observed value. Permutation testing was conducted using custom written code in R.

2.3 Results

Properties of Animals, Dendrites, and Spines

Table 1 lists aggregate properties of the mice, dendrites, and spines imaged in RSC for both trained and control groups. Similar numbers of spines and dendritic segments were counted for both trained and control animals. Additionally, the spine density was similar for both trained and control animals on the first imaging day (BL1) and on the final day of imaging (LCD5).

Table 1: Properties of Animals, Dendrites and Spines in RSC

	Trained	Control
Number of Animals	18	18
Total Length of Dendrite (μm)	13323.31	14498.32
Number of Dendritic Segments	593	573
Dendritic Segments per animal (mean ± s.e.m.)	33.10 ± 3.51	31.83 ± 4.99
Total Number of Spines at BL1	6438	7062
Total Number of Spines at LCD5	6429	7042
Spine Density at BL1 (spines/μm) (mean ± s.e.m.)	0.39 ± 0.01	0.39 ± 0.01
Spine Density at LCD5 (spines/μm) (mean ± s.e.m.)	0.39 ± 0.01	0.39 ± 0.01
BL1=Baseline Day 1; LCD5=Learning Curve Day 5		

Behavioral Data

Thy1-YFP mice demonstrated a gradual increase in context freezing over the course of five days of contextual fear conditioning (Day 2: mean=1.962%, s.e.m.=1.045%; Day 3: mean=19.753%, s.e.m.=4.585%; Day 4: mean=23.627%, s.e.m.=5.680%; Day 5: mean=23.279%, s.e.m.=4.845%) (Figure 2.2). No freezing behavior was detected in any animal on the first day of conditioning (Baseline) before shock administration.

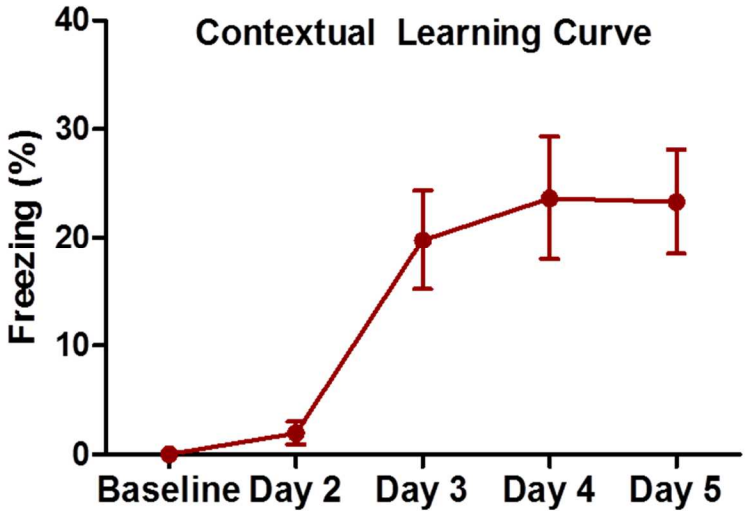

Figure 2.2: Repeated contextual fear conditioning generates a learning curve.
Mild contextual fear conditioning repeated daily causes a gradual increase in context freezing. n=18 mice. Data shown are mean ± s.e.m

Dendritic Spine Gain and Loss

Segments of dendrite were chosen randomly for imaging on the first day of baseline imaging. At each successive imaging day the same segments of dendrite were located and re-imaged so that four imaging time points were acquired (Baseline 1, Baseline 2, Learning Day 2, and Learning Day 5 (Figure 2.3A). Following completion of all imaging sessions, spine dynamics were analyzed by assessing the presence, loss, or gain of spines on each segment of dendrite.

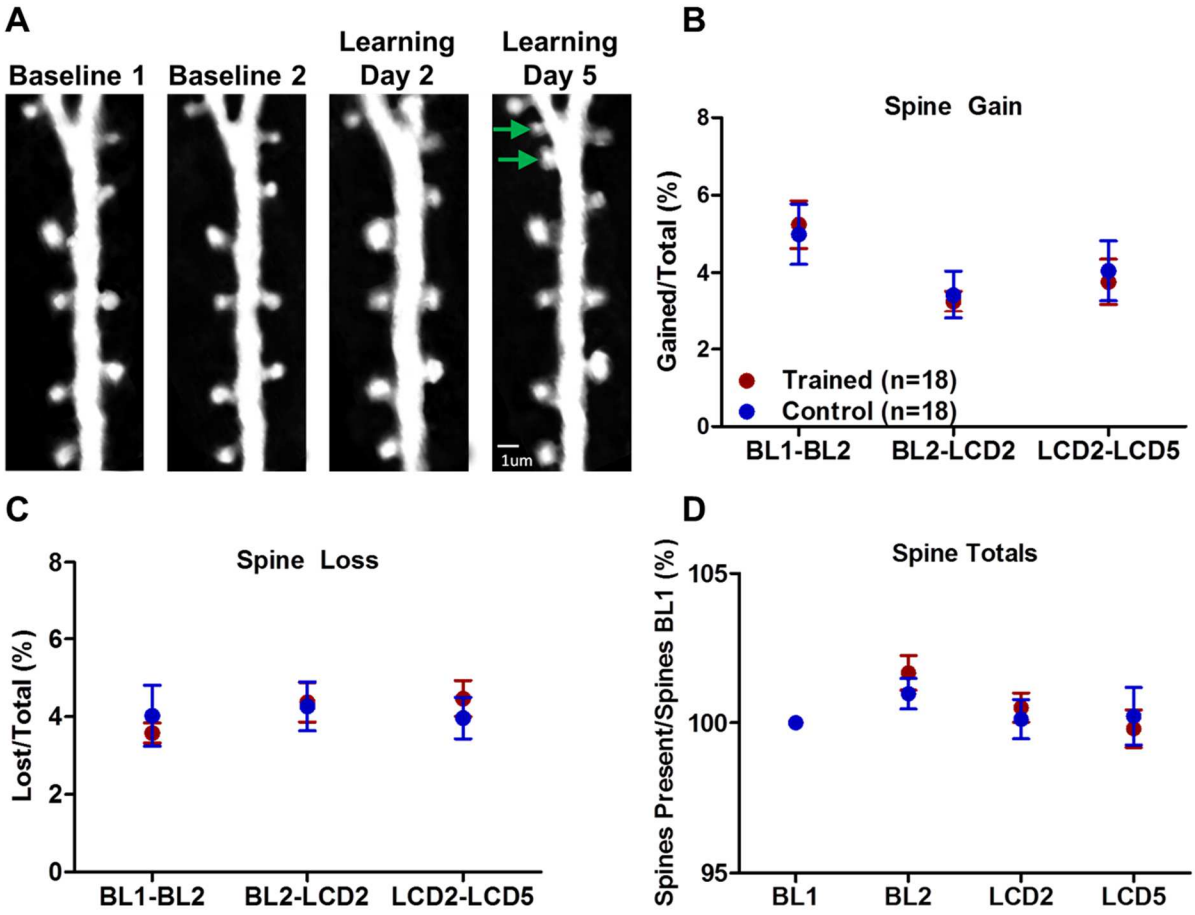

Figure 2.3: Gain and Loss of Dendritic Spines.
(A) Representative example of repeated imaging of the same segment of dendrite at four time points. Green arrows indicate addition of two new spines by the final imaging session. (B) The percentage of newly added spines did not differ between trained and control animals at each imaging time point. (C) The percentage of lost spines did not differ between trained and control animals at each imaging time point. (D) The total number of spines present as a percentage of spines present at baseline 1 imaging does not differ between trained and control animals at each imaging point. Data shown are mean ± s.e.m. BL1-BL2, baseline 1-baseline 2; BL2-LCD2, baseline 2-learning curve day 2; LCD2-LCD5, learning curve day2-learning curve day 5. Scale bar in (A) is 1 μm.

No difference existed between animals trained in contextual fear conditioning and home cage control animals for the percentage of spines gained between baseline 1 and baseline 2 (trained: mean=5.251%, s.e.m.=0.615%; control: mean=4.993%, s.e.m.=0.7765; Mann Whitney, U=141.4, p=0.527), between baseline 2 and learning curve day 2 (trained: mean=3.233%, s.e.m.=0.257%; control: mean=3.425%, s.e.m.=0.618%; Mann Whitney, U=136.5, p=0.429), or between learning curve day 2 and learning curve day 5 (trained: mean=3.795%, s.e.m.=0.601%; control: mean=4.050%, s.e.m.=0.773%; Mann Whitney, U=158.0, p=0.912) (Figure 2.3B). Further, no difference existed between trained and control animals for the percentage of spines

lost between baseline 1 and baseline 2 (trained: mean=3.588%, s.e.m.=0.260%; control: mean=4.023%, s.e.m.=0.785%; Mann Whitney, U=161.0, p=0.987), between baseline 2 and learning curve day 2 (trained: mean=4.330%, s.e.m.=0.506%; control: mean=4.265%, s.e.m.=0.631%; Mann Whitney, U=158.0, p=0.912), or between learning curve day 2 and learning curve day 5 (trained: mean=4.480%, s.e.m.=0.484%; control: mean=3.961%, s.e.m.=0.533%; Mann Whitney, U=130.0, p=0.319) (Figure 2.3C). Finally, the total number of spines present as a percentage of the total number of spines on baseline 1 did not differ between trained and control animals at baseline 2 (trained: mean=101.7%, s.e.m.=0.570%; control: mean=101.0%, s.e.m.=0.510%; Mann Whitney, U=140.0, p=0.496), at learning curve day 2 (trained: mean=100.5%, s.e.m.=0.491%; control: mean=100.1%, s.e.m.=0.650%; Mann Whitney, U=152.0, p=0.764), or at learning curve day 5 (trained: mean=99.84%, s.e.m.=0.630%; control: mean=100.2%, s.e.m.=0.958%; Mann Whitney, U=160.0, p=0.926) (Figure 2.3D).

Clustered Addition of Dendritic Spines

While no differences existed between animals undergoing contextual fear conditioning and home cage control animals in the percentage of spines gained or lost or the total number of spines present (Figure 2.3B,C,D), analysis of where new spines were added during learning revealed a significant difference between groups. Specifically, we analyzed new spines that were added during training near each other and found that a significantly greater percentage of new spines occurred in clusters within 5um of each other in trained (mean=42.83%, s.e.m.=2.718%) versus control mice (mean=21.94%, s.e.m.=3.661%) (Mann Whitney, U=51.00, p=0.0005) (Figure 2.4A).

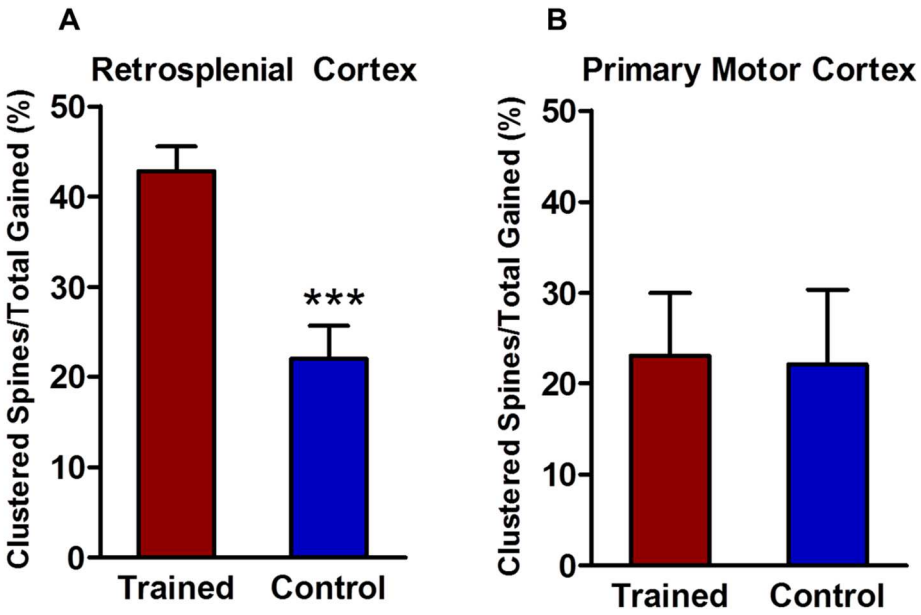

Figure 2.4: Clustered addition of dendritic spines occurs in retrosplenial cortex.
(A) Animals trained in contextual fear conditioning have a higher percentage of new spines in retrosplenial cortex added in clusters within 5μm of each other than home cage control animals. Trained, n=18 mice; control, n=18 mice (B) No difference exists in the percentage of new spines occurring in clusters between trained and home cage control animals if spines are imaged in primary motor cortex. Trained, n=7; control, n=7. Data shown are mean ± s.e.m. ***, $p<0.001$.

This finding is specific for retrosplenial cortex as no difference in the percentage of new spines occurring in clusters (within 5μm of each other) exists between trained (mean=23.02%, s.e.m.=6.949%) and control (mean=22.05%, s.e.m.=8.309%) animals when dendritic spines are imaged in primary motor cortex (Mann Whitney, U=24.00, p=1.0) (Figure 2.4B).

Properties of Clustered Spines

Contextual fear conditioning induced a significant increase in the percentage of new spines added in clusters in RSC. Table 2 displays properties of clustered spines for trained and control animals. While trained animals had more new spines in clusters, the number of clustered spines per segment, the number of clusters per segment, and the percentage of dendritic segments with clusters were similar between trained and control animals.

Table 3 displays the size and shape of clusters of new spines in both trained and control animals imaged in RSC. Approximately half of all clusters formed as two new spines immediately next to each other and within 5 μm of each other. Approximately half of all clusters

formed with existing stable spines intervening between the newly added spines. The majority of clustered spines formed in clusters of two new spines. The remaining clusters consisted of three or four new spines appearing within 5 μm of each other. While trained animals had more new spines added in clusters, the number of spines in a cluster and the cluster shape were similar between trained and control animals.

Table 2: Properties of Clustered Spines

	Trained (n=18 mice)	Control (n=18 mice)
Number of New, Stable Spines	385	381
Number of Clustered Spines	175	110
Percentage of Clustered Spines	45%	29%
Number of Clusters per segment on segments with clusters (mean ± s.e.m.)	1.24 ± 0.06	1.19 ± 0.09
Number of segments with clusters	63	43
Percentage of segments with clusters	11%	8%
Number of segments with >1 cluster	13	5
Number of clustered spines per segment (mean ± s.e.m.)	2.76 ± 0.15	2.63 ± 0.19
Distance between clusters on same segment (μm) (mean ± s.e.m.)	18.93 ± 3.05	13.70 ± 2.12

Table 3: Properties of Cluster Size and Cluster Shape

Number of Spines in Cluster	Cluster Configurations	Number of Cases	
		Trained	Control
2	N-N	31	26
	N-S-N	24	10
	N-S-S-N	6	3
	N-S-S-S-N	1	2
	Total	62	41
	Percentage of all clusters	79%	82%
	Percentage of clustered spines	71%	75%
3	N-N-N	8	2
	N-N-S-N	1	3
	N-N-S-S-N	1	1
	N-S-N-S-N	1	2
	N-S-N-S-S-N	1	0
	N-S-N-S-S-S-N	1	0
	Total	13	8
	Percentage of all clusters	17%	16%
	Percentage of clustered spines	22%	22%
4	N-N-N-N	0	1
	N-N-S-S-N-N	1	0
	N-S-N-N-S-S-N	1	0
	N-S-N-S-S-S-N-N	1	0
	Total	3	1
	Percentage of all clusters	4%	2%
	Percentage of clustered spines	7%	4%
N=New, clustered spine; S=Existing, stable spine			

Permutation Analysis of Spine Clustering

Permutation analysis of spine clustering in trained animals was conducted for each segment of dendrite for each animal and results were pooled. The number of new spines

gained during learning for each segment was assessed and this number of used to permute the spine types for all spines on this segment (i.e. if three spines were added during learning to a given segment and 15 total spines exist on that segment, for each permutation, three of the 15 spines would randomly be assigned as new spines).

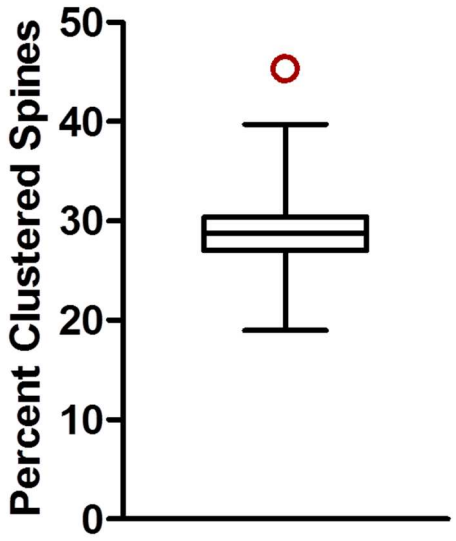

Figure 2.5: Permutation analysis of spine clustering. The percentage of clustered new spines was significantly greater than chance. 100,000 permutations of spine distributions were run based on the number of spines and dendritic length measured, and the percent of new spines within 5 μm of each other was calculated. The median permutation value is shown. The box represents the interquartile range and whiskers represent the minimum and maximum permutation values. The circle represents the actual percentage of clustered spines observed from the data. The exact p-value is 0, as no permutation values were equal to or more extreme than our observed data.

Clustering was assessed for each permutation as the percentage of new spines gained during learning that existed within 5μm of each other. This was calculated for all segments of dendrite across all animals for each permutation. One hundred thousand permutations were conducted; a minimum of 18.96% clustering and a maximum of 39.74% clustering occurred with a median of 28.83%. The observed value of clustering from the data using this segment-wise analysis was 45.45% (Figure 2.5). The exact p-value is zero as no permutation values were equal to or greater than the observed clustering percentage.

Clustered Spine Survival

New spine survival rate in the adult animal is variable but generally low (Holtmaat and Svoboda, 2009). We assessed survival of spines added during contextual fear conditioning by imaging a subset of trained animals (n=10 mice) four to six weeks after the end of contextual fear training (Figure 2.6A). We found that new spines that were added in clusters had a

significantly higher survival rate (mean=69.60%, s.e.m.=4.77%) than new spines not added in a clustered fashion (mean=49.83%, s.e.m.=3.10%, Mann Whitney, U=10.50, p=0.0029) (Figure 2.6B).

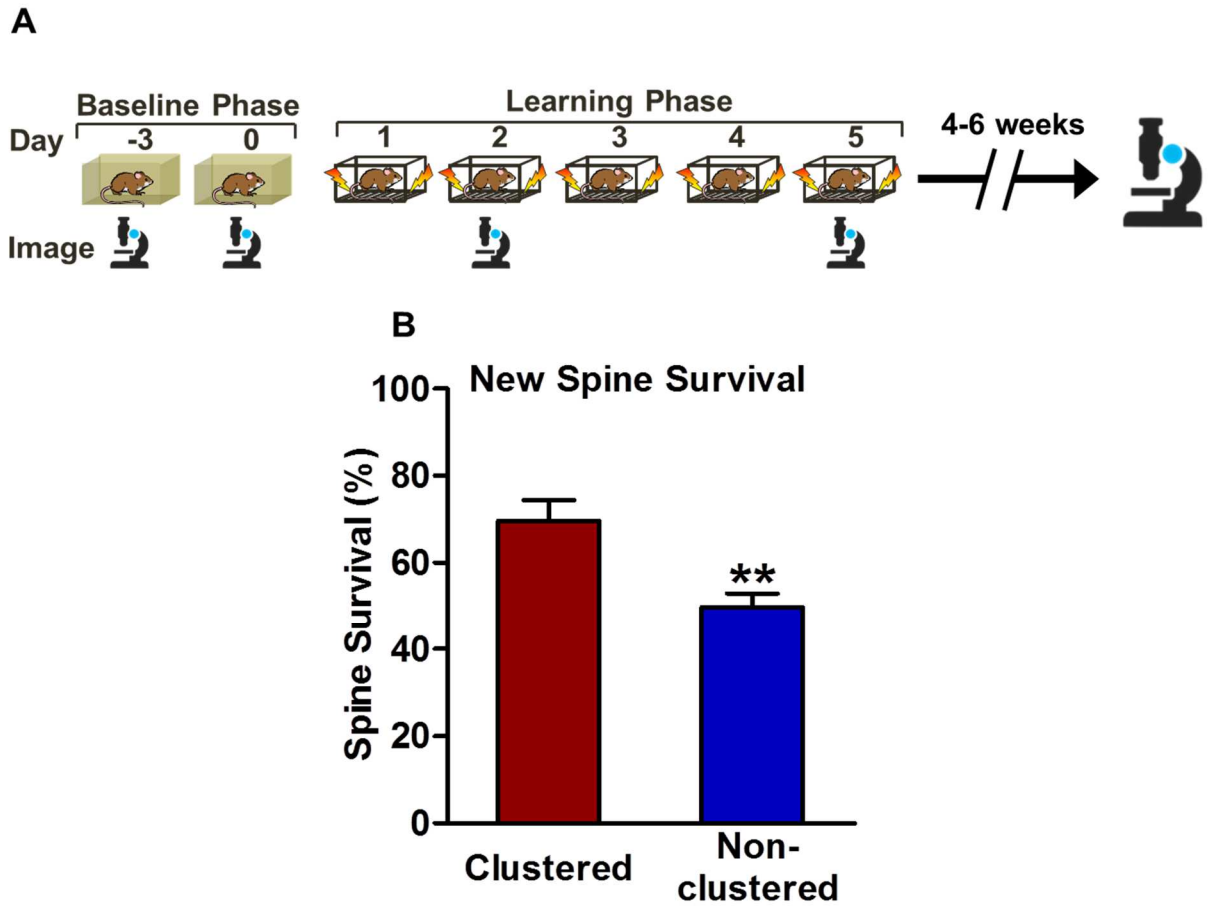

Figure 2.6: New spine survival one month after learning.
(A) A subset of animals was imaged four to six weeks after the end of contextual fear conditioning. The same segments of dendrite imaged during learning were re-imaged at this remote time point to allow for assessment of the presence or absence of spines. (B) New spines added during contextual fear conditioning in clusters (n=119 spines in 10 mice) had significantly higher survival rates than new spines that were not added in clusters (n=120 spines in 10 mice). Data shown are mean ± s.e.m. **, p<.01.

Clustered Addition of Spines Correlates with Learning

Analysis of the correlation between the percentage of newly added clustered spines and learning was conducted in two ways: learning was assessed both as the percentage of time mice froze before shock administration averaged over all learning days or as the slope of the

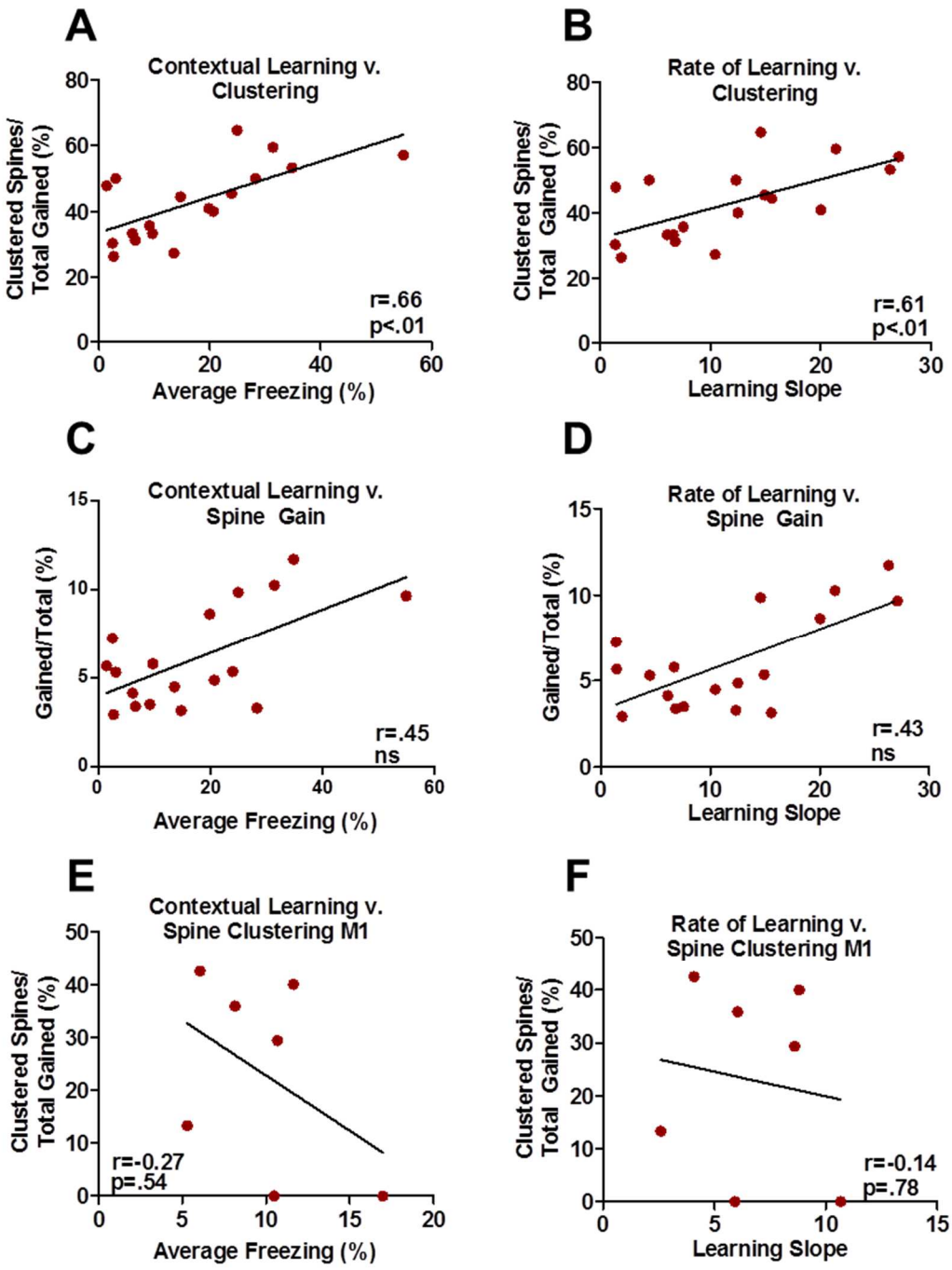

Figure 2.7: Clustered spine addition correlates with behavioral performance.

(A) Freezing behavior averaged over all testing days (day 2 – day 5) correlates with the percentage of new spines added in clusters within 5 μm of each other during learning in retrosplenial cortex. n=18 mice. (B) Rate of learning, assessed as the slope of the line from baseline freezing to asymptotic freezing, correlates with the percentage of new spines added in clusters during learning in retrosplenial cortex. n=18 mice, same animals as in (A). (C) Average freezing does not correlate with the total percentage of spines gained during learning. n=18 mice, same animals as in (A). (D) Rate of learning does not correlate with the total percentage of spines gained during learning. n=18 mice, same animals as in (A). (E) Average freezing does not correlate with percentage of new spines added in clusters during learning in primary motor cortex. n=7 mice. (F) Rate of learning does not correlate with the percentage of new spines added in clusters during learning in primary motor cortex. n=7 mice, same animals as in (E). Spearman's rho.

learning curve for each mouse. A significant positive correlation exists between clustered spine addition during contextual fear conditioning and average freezing behavior (Spearman's rho, r=0.662, p=0.0028) (Figure 2.7A). Additionally, a significant positive correlation exists between clustered spine addition during contextual fear conditioning and learning rate (Spearman's rho, r=0.607, p=0.0075) (Figure 2.7B). No significant correlation was found between the percentage of total spines gained during contextual fear conditioning for either average freezing (Spearman's rho, r=0.447, p=0.063) (Figure 2.7C) or for learning rate (Spearman's rho, r=0.430, p=0.075) (Figure 2.7D). Finally, no significant correlation was found between clustered spine addition in primary motor cortex during contextual fear conditioning for either average freezing (Spearman's rho, r= - 0.27, p=0.556) (Figure 2.7E) or for learning rate (Spearman's rho, r=-0.14, p=0.783) (Figure 2.7F).

2.4 Discussion

We aimed to examine if clustered structural plasticity in the form of clustered dendritic spine addition is a general property of cortical pyramidal cells during learning. To do this we utilized chronic *in vivo* two-photon imaging of the apical dendrites of layer 5 pyramidal neurons in mouse RSC at baseline and while animals underwent contextual fear conditioning. The RSC is a brain region critically involved in spatial learning and memory (Vann et al., 2009), and specifically activated by and required for contextual fear conditioning (Keene and Bucci, 2008; Corcoran et al., 2011; Robinson et al., 2012; Cowansage et al., 2014). As RSC is required for both recent and remote spatial memory (Corcoran et al., 2011), we postulated that structural changes, such as clustered dendritic spine addition, might be observed as animals learn a spatial memory task.

While dendritic spines are largely stable in adult mice, spine dynamics are modifiable with sensory deprivation (Holtmaat et al., 2006; Hofer et al., 2009), sensory organ lesion (Keck

et al., 2008), environmental enrichment (Jung and Herms, 2012), and learning (Moczulska et al., 2013; Xu et al., 2009). We were thus surprised to find that basic properties of dendritic spines in retrosplenial cortex - such as the percentage of gained spines, the percentage of lost spines, the total number of spines, and spine density – were not altered in 3-6 month old mice due to contextual fear conditioning. One possibility why we did not observe alterations to the rate of gain and loss of spines due to fear conditioning is that the aforementioned studies reporting such changes were conducted in primary sensory or motor cortices. It is therefore possible that a multimodal association area such as the RSC does not show gross changes to rate of gain or loss of spines or total spine number. However, Lai *et al* found that spines in frontal association cortex were lost at an increased rate due to tone fear conditioning and gained at an increased rate due to tone fear extinction (Lai et al., 2012). These studies, however, were conducted in one-month-old adolescent mice which are known to have higher baseline rates of spine addition and elimination than adult animals utilized in our studies (Zuo et al., 2005). It is possible that adolescent cortex is primed to respond to learning with larger changes to spine gain and loss than the adult brain. Another possible reason we did not see changes in spine number, rate of addition, or rate of elimination between trained and control animals is that imaging was not conducted frequently enough. Specifically, studies have found that changes to the rate of spine gain or loss due to learning (Xu et al., 2009; Moczulska et al., 2013) and brief sensory deprivation (Yu et al., 2011) are rapid and often transient. Thus, it is possible that these changes also occur in RSC following learning, but that we did not have the temporal resolution to witness them due to our imaging schedule (i.e. animals undergoing fear conditioning experience an increase in the rate of spine gain – or loss – for the day immediately following commencement of training, but that rates of gain/loss return to baseline levels as training progresses).

While contextual fear conditioning did not alter the rate of gain or loss of spines or the total number of spines present, we did find that learning altered where new spines occurred.

Specifically, new spines added in RSC during the learning phase of imaging were significantly more likely to occur in clusters within 5 μm of each other in animals undergoing contextual fear conditioning compared to home cage controls. The 5 μm window was chosen for analysis as biochemical studies of clustered plasticity demonstrate diffusion of molecules between spines within this distance (Harvey and Svoboda, 2007; Harvey et al., 2008; Murakoshi et al., 2011). Our findings support and extend work conducted in primary motor cortex which demonstrated that animals who learn a seed-reaching task have a significant increase in the percentage of new dendritic spines added in clusters (Fu et al., 2012). Our results indicate that clustered spine addition during learning is not a phenomenon confined to motor cortex or to motor learning, but is also present in association cortex and due to episodic-like learning. We also demonstrate that spine clustering during spatial learning is specific for RSC - a structure critical for acquisition and storage of contextual fear memories – by showing that there is no increase in the percentage of clustered spines in primary motor cortex due to contextual fear conditioning. This finding also demonstrates that the contextual fear conditioning protocol and associated foot shock do not alter spine dynamics and spine clustering non-specifically throughout the cortex.

To assess for the possibility that the percentage of clustered spine addition witnessed in trained animals is due to chance, we conducted a permutation analysis of the data. In this analysis, the number of new spines was assessed, this number was used to randomly select a sample population of spines chosen from all spines present on a segment of dendrite, and these spines were then tested to see if they existed within 5 μm of each other (i.e. were clustered). This process was repeated 100,000 times and resulted in a distribution of clustering percentages. We found that the percentage of spines occurring in clusters in trained animals was greater than any value obtained by permutation, supporting the conjecture that the clustered spine addition we witnessed due to spatial learning was not simply due to chance.

Most existing spines in adult cortex are stable, while newly added spines show a much lower survival rate (Trachtenberg et al., 2002; Holtmaat et al., 2005; Grutzendler et al., 2002;

Holtmaat et al., 2009). It has also been demonstrated that learning destabilizes existing spines (i.e. pre-existing spines have a lower survival rate in animals undergoing a learning task) while increasing the survival rate of spines added during learning (Xu et al., 2009). Additionally, Fu *et al* found that spines added in clusters during motor learning had a further increase in stability (Fu et al., 2012). To examine if newly added clustered spines in RSC also showed a difference in long-term stability from new non-clustered spines, we re-imaged animals approximately one month after fear conditioning ended. In agreement with data from motor cortex, we found that new spines added in clusters during learning had a significant increase in stability. Both motor learning and contextual fear conditioning result in stable long term memories (Xu et al., 2009; Gale et al., 2004) and it is possible that clustered spine addition represents a structural trace of this long term memory storage.

In further support for the role of clustered spine addition in memory formation, we found a strong correlation between the percentage of clustered spines and two proxies for learning: average freezing and rate of learning. This result was all the more striking considering that clustered spines were on average only 2.5% of the total spine population assessed in each mouse. Though there is no significant correlation between total spine gain and memory (assessed either as average freezing or rate of learning), there is a trend, which suggests that total spine gain in RSC may itself be important for contextual fear conditioning. These novel results are the first *in vivo* demonstration of a correlation between spine clustering and any measure of behavior or memory. Further these results demonstrate that clustered structural plasticity occurs following formation of episodic-like memory.

2.5 References

Amin, E., Pearce, J. M., Brown, M. W., & Aggleton, J. P. (2006). Novel temporal configurations of stimuli produce discrete changes in immediate-early gene expression in the rat hippocampus. European Journal of Neuroscience, 24(9), 2611–2621.

Chen, L. L., Lin, L. H., Green, E. J., Barnes, C. A., & McNaughton, B. L. (1994). Head-direction cells in the rat posterior cortex. I. Anatomical distribution and behavioral modulation. Experimental Brain Research. Experimentelle Hirnforschung. Experimentation Cerebrale, 101, 8–23.

Cho, J., & Sharp, P. E. (2001). Head direction, place, and movement correlates for cells in the rat retrosplenial cortex. Behavioral Neuroscience, 115, 3–25.

Cooper, B. G., & Mizumori, S. J. (2001). Temporary inactivation of the retrosplenial cortex causes a transient reorganization of spatial coding in the hippocampus. The Journal of Neuroscience : The Official Journal of the Society for Neuroscience, 21(11), 3986–4001.

Corcoran, K. A., Donnan, M. D., Tronson, N. C., Guzman, Y. F., Gao, C., Jovasevic, V., … Radulovic, J. (2011). NMDA Receptors in Retrosplenial Cortex Are Necessary for Retrieval of Recent and Remote Context Fear Memory. Journal of Neuroscience, 31(32), 11655–11659.

Cowansage, K. K., Shuman, T., Dillingham, B. C., Chang, A., Golshani, P., & Mayford, M. (2014). Direct Reactivation of a Coherent Neocortical Memory of Context. Neuron, 84(2), 432–441.

Czajkowski, R., Jayaprakash, B., Wiltgen, B., Rogerson, T., Guzman-Karlsson, M. C., Barth, A. L., Trachtenberg, J., Silva, A. J. (2014). Encoding and storage of spatial information in the retrosplenial cortex. Proceedings of the National Academy of Sciences of the United States of America, 111(23), 8661–6.

Frankland, P. W., & Bontempi, B. (2005). The organization of recent and remote memories. Nat Rev Neurosci, 6(2), 119–130.

Fu, M., Yu, X., Lu, J., & Zuo, Y. (2012). Repetitive motor learning induces coordinated formation of clustered dendritic spines in vivo. Nature, 483(7387), 92–5.

Gale, G. D., Anagnostaras, S. G., Godsil, B. P., Mitchell, S., Nozawa, T., Sage, J. R., … Fanselow, M. S. (2004). Role of the basolateral amygdala in the storage of fear memories across the adult lifetime of rats. The Journal of Neuroscience : The Official Journal of the Society for Neuroscience, 24(15), 3810–3815.

Govindarajan, A., Israely, I., Huang, S.-Y., & Tonegawa, S. (2011). The Dendritic Branch Is the Preferred Integrative Unit for Protein Synthesis-Dependent LTP. Neuron, 69(1), 132–146.

Govindarajan, A., Kelleher, R. J., & Tonegawa, S. (2006). A clustered plasticity model of long-term memory engrams. Nature Reviews. Neuroscience, 7(7), 575–83.

Grutzendler, J., Kasthuri, N., & Gan, W.-B. (2002). Long-term dendritic spine stability in the adult cortex. Nature, 420(6917), 812–6.

Han, J.-H., Kushner, S. A., Yiu, A. P., Hsiang, H.-L. L., Buch, T., Waisman, A., … Josselyn, S. A. (2009). Selective erasure of a fear memory. Science (New York, N.Y.), 323, 1492–1496.

Harker, K. T., & Whishaw, I. Q. (2004). Impaired place navigation in place and matching-to-place swimming pool tasks follows both retrosplenial cortex lesions and cingulum bundle lesions in rats. Hippocampus, 14, 224–231.

Harvey, C. D., & Svoboda, K. (2007). Locally dynamic synaptic learning rules in pyramidal neuron dendrites. Nature, 450(7173), 1195–200.

Harvey, C. D., Yasuda, R., Zhong, H., & Svoboda, K. (2008). The spread of Ras activity triggered by activation of a single dendritic spine. Science (New York, N.Y.), 321(5885), 136–40.

Hofer, S. B., Mrsic-Flogel, T. D., Bonhoeffer, T., & Hübener, M. (2009). Experience leaves a lasting structural trace in cortical circuits. Nature, 457(7227), 313–7.

Holtmaat, A., Bonhoeffer, T., Chow, D. K., Chuckowree, J., De Paola, V., Hofer, S. B., … Wilbrecht, L. (2009). Long-term, high-resolution imaging in the mouse neocortex through a chronic cranial window. Nat. Protocols, 4(8), 1128–1144.

Holtmaat, A. J. G. D., Trachtenberg, J. T., Wilbrecht, L., Shepherd, G. M., Zhang, X., Knott, G. W., & Svoboda, K. (2005). Transient and persistent dendritic spines in the neocortex in vivo. Neuron, 45(2), 279–91.

Holtmaat, A., Wilbrecht, L., Knott, G. W., Welker, E., & Svoboda, K. (2006). Experience-dependent and cell-type-specific spine growth in the neocortex. Nature, 441(7096), 979–83.

Jones, B. F., Groenewegen, H. J., & Witter, M. P. (2005). Intrinsic connections of the cingulate cortex in the rat suggest the existence of multiple functionally segregated networks. Neuroscience, 133, 193–207.

Jung, C. K. E., & Herms, J. (2012). Structural Dynamics of Dendritic Spines are Influenced by an Environmental Enrichment: An In Vivo Imaging Study. Cerebral Cortex (New York, N.Y. : 1991), 24, 377–384.

Keck, T., Mrsic-Flogel, T. D., Vaz Afonso, M., Eysel, U. T., Bonhoeffer, T., & Hübener, M. (2008). Massive restructuring of neuronal circuits during functional reorganization of adult visual cortex. Nature Neuroscience, 11(10), 1162–7.

Keene, C. S., & Bucci, D. J. (2008). Contributions of the retrosplenial and posterior parietal cortices to cue-specific and contextual fear conditioning. Behav Neurosci, 122(1), 89–97.

Lai, C. S. W., Franke, T. F., & Gan, W.-B. (2012). Opposite effects of fear conditioning and extinction on dendritic spine remodelling. Nature, 483(7387), 87–91.

Lukoyanov, N. V., & Lukoyanova, E. A. (2006). Retrosplenial cortex lesions impair acquisition of active avoidance while sparing fear-based emotional memory. Behavioural Brain Research, 173, 229–236.

Majewska, A. K., Newton, J. R., & Sur, M. (2006). Remodeling of synaptic structure in sensory cortical areas in vivo. The Journal of Neuroscience : The Official Journal of the Society for Neuroscience, 26(11), 3021–3029.

McBride, T. J., Rodriguez-Contreras, A., Trinh, A., Bailey, R., & Debello, W. M. (2008). Learning drives differential clustering of axodendritic contacts in the barn owl auditory system. The Journal of Neuroscience : The Official Journal of the Society for Neuroscience, 28(27), 6960–73.

Moczulska, K. E., Tinter-Thiede, J., Peter, M., Ushakova, L., Wernle, T., Bathellier, B., & Rumpel, S. (2013). Dynamics of dendritic spines in the mouse auditory cortex during memory formation and memory recall. Proceedings of the National Academy of Sciences of the United States of America, 110(45), 18315–20.

Morris, R., Pandya, D. N., & Petrides, M. (1999). Fiber system linking the mid-dorsolateral frontal cortex with the retrosplenial]presubicular region in the rhesus monkey. Journal of Comparative Neurology, 407, 183–192.

Murakoshi, H., Wang, H., & Yasuda, R. (2011). Local, persistent activation of Rho GTPases during plasticity of single dendritic spines. Nature, 472(7341), 100–4.

Poirazi, P., & Mel, B. W. (2001). Impact of active dendrites and structural plasticity on the memory capacity of neural tissue. Neuron, 29(3), 779–96.

Pothuizen, H. H. J., Davies, M., Albasser, M. M., Aggleton, J. P., & Vann, S. D. (2009). Granular and dysgranular retrosplenial cortices provide qualitatively different contributions to spatial working memory: evidence from immediate-early gene imaging in rats. European Journal of Neuroscience, 30(5), 877–888.

Reijmers, L. G., Perkins, B. L., Matsuo, N., & Mayford, M. (2007). Localization of a Stable Neural Correlate of Associative Memory. Science, 317(5842), 1230–1233.

Robinson, S., Poorman, C., Marder, T., & Bucci, D. J. (2012). Identification of Functional Circuitry between Retrosplenial and Postrhinal Cortices during Fear Conditioning. The Journal of Neuroscience, 32(35), 12076–12086.

Silva, A. J., Zhou, Y., Rogerson, T., Shobe, J., & Balaji, J. (2009). Molecular and Cellular Approaches to Memory Allocation in Neural Circuits. *Science*, *326*(5951), 391–395.

Smith, D., Barredo, J., & Mizumori, S. (2011). Complimentary Roles of the Hippocampus and Retrosplenial Cortex in Behavioral Context Discrimination. Hippocampus.

St-Laurent, M., Petrides, M., & Sziklas, V. (2009). Does the cingulate cortex contribute to spatial conditional associative learning in the rat? Hippocampus, 19, 612–622.

Sutherland, R. J., Whishaw, I. Q., & Kolb, B. (1988). Contributions of Cingulate Cortex to 2 Forms of Spatial-Learning and Memory. Journal of Neuroscience, 8(6), 1863–1872.

Tabuchi, E., Furusawa, A. A., Hori, E., Umeno, K., Ono, T., & Nishijo, H. (2005). Neural correlates to action and rewards in the rat posterior cingulate cortex. Neuroreport, 16, 949–953.

Taube, J. S. (2007). The head direction signal: origins and sensory-motor integration. Annual Review of Neuroscience, 30, 181–207.

Trachtenberg, J. T., Chen, B. E., Knott, G. W., Feng, G. P., Sanes, J. R., Welker, E., & Svoboda, K. (2002). Long-term in vivo imaging of experience-dependent synaptic plasticity in adult cortex. Nature, 420(6917), 788–794.

Van Groen, T., & Wyss, J. M. (1990). Connections of the retrosplenial granular a cortex in the rat. The Journal of Comparative Neurology, 300, 593–606.

Van Groen, T., & Wyss, J. M. (1992). Connections of the retrosplenial dysgranular cortex in the rat. The Journal of Comparative Neurology, 315(2), 200–16.

Van Groen, T., & Wyss, J. M. (2003). Connections of the retrosplenial granular b cortex in the rat. Journal of Comparative Neurology, 463, 249–263.

Vann, S. D., & Aggleton, J. P. (2002). Extensive cytotoxic lesions of the rat retrosplenial cortex reveal consistent deficits on tasks that tax allocentric spatial memory. Behav Neurosci, 116(1), 85–94.

Vann, S. D., Aggleton, J. P., & Maguire, E. A. (2009). What does the retrosplenial cortex do? Nat Rev Neurosci, 10(11), 792–802.

Vann, S. D., Brown, M. W., & Aggleton, J. P. (2000). Fos expression in the rostral thalamic nuclei and associated cortical regions in response to different spatial memory tests. Neuroscience, 101(4), 983–991.

Vann, S. D., Wilton, L. A. K., Muir, J. L., & Aggleton, J. P. (2003). Testing the importance of the caudal retrosplenial cortex for spatial memory in rats. Behavioural Brain Research, 140(1-2), 107–118.

Vogt, B. a. (1985). Association and Auditory Cortices. In A. Peters & E. Jones (Eds.), Cerebral Cortex (Vol. 4, pp. 89–149). New York: Plenum.

Vogt, B. a, & Paxinos, G. (2012). Cytoarchitecture of mouse and rat cingulate cortex with human homologies. Brain Structure & Function, (1909).

Vogt, B. A., & Miller, M. W. (1983). Cortical connections between rat cingulate cortex and visual, motor, and postsubicular cortices. The Journal of Comparative Neurology, 216, 192–210.

Whishaw, I. Q., Maaswinkel, H., Gonzalez, C. L., & Kolb, B. (2001). Deficits in allothetic and idiothetic spatial behavior in rats with posterior cingulate cortex lesions. Behavioural Brain Research, 118, 67–76.

Xu, T., Yu, X., Perlik, A. J., Tobin, W. F., Zweig, J. a, Tennant, K., … Zuo, Y. (2009). Rapid formation and selective stabilization of synapses for enduring motor memories. Nature, 462(7275), 915–9.

Yu, H., Majewska, A. K., & Sur, M. (2011). Rapid experience-dependent plasticity of synapse function and structure in ferret visual cortex in vivo. Proceedings of the National Academy of Sciences, 108(52), 21235–21240.

Zhou, Y., Won, J., Karlsson, M. G., Zhou, M., Rogerson, T., Balaji, J., … Silva, A. J. (2009). CREB regulates excitability and the allocation of memory to subsets of neurons in the amygdala. Nat Neurosci, 12(11), 1438–1443.

Zuo, Y., Lin, A., Chang, P., & Gan, W.-B. (2005). Development of long-term dendritic spine stability in diverse regions of cerebral cortex. Neuron, 46(2), 181–9.

Chapter 3

Learning Alters the Spatial Distribution of Dendritic Spines

3.1 Introduction

Structural clustered plasticity in the form of clustered spine formation is postulated to serve as a mechanism for memory formation and storage and as a means to increase storage capacity in neural circuits (Poirazi and Mel, 2001; Govindarajan et al., 2006; Fu et al., 2012). In addition to clustered spine gain, spatially restricted spine loss has also been observed due to electrical stimulation and learning, and has the potential to influence computation within neurons (Wiegert and Oertner, 2013; Lai et al., 2012).

First, Wiegert *et al* observed a spatial interaction of dendritic spine loss following LTD. Specifically, the authors induced LTD between Schaffer collaterals and CA1 neurons via low frequency optogenetic stimulation of Channelrhodopsin expressing CA3 neurons. CA1 cells expressed both GCaMP3 - to monitor calcium dynamics in individual spines - and cerulean - to assess dendrite and spine morphology. Spines responsive to test pulses before LTD induction and fluorescently verified to have undergone depression after LTD were preferentially lost within seven days. Further, non-responsive spines neighboring a depressed spine (within 8 μm) were also lost at a higher rate by day 7 then spines not near a depressed synapse. These results demonstrate a spatial interaction between spines lost following LTD and nearby spine. This is similar, though opposite in nature, to the facilitation of LTP at spines near recently potentiated

spines (Harvey and Svoboda, 2007; Harvey et al., 2008), and suggests that a diffusible molecule may be mediating this clustered spine loss.

In addition to clustered spine loss, spatial interaction of gain and loss has also been observed. Specifically, Lai *et al* utilized chronic *in vivo* imaging in frontal association cortex and found that tone fear conditioning causes spine loss while extinction of this memory causes spine gain (Lai et al., 2012). Interestingly, if, following extinction, animals are reconditioned to the original tone, spines formed during extinction have a lower survival rate if they lie within 2 μm of a spine lost during conditioning. While a single diffusible molecule is unlikely to explain these complicated interactions between nearby spines, these results demonstrate that induction of structural plasticity influences the region in which it occurs, making it more likely for subsequent plasticity to occur nearby.

Given the spatial interaction and restriction of spine loss due to LTD seen by Wiegert *et al* and the spatial interaction of spine gain and loss seen by Lai *et al*, we were interested in examining spine loss in our data set. While we see no difference in the percentage of spines lost in animals undergoing contextual fear conditioning compared to home cage controls, we sought to determine if learning impacts where spines are lost; we thus assessed the spatial distribution of spine loss in trained and control animals. Further, we were interested in interactions that might occur between clustered gained spines and lost spines and thus examined the spatial distribution of gained and lost spines.

3.2 Methods

Surgery and Cranial Window Placement

Surgery and cranial window placement were conducted as in section 2.2.

Animals

The same animals imaged for spine dynamics in RSC from section 2.2 were utilized herein.

Behavioral Paradigm

Animals were handled and contextually fear conditioned as in section 2.2. Assessment of freezing and calculation of average freezing and learning slope were conducted as in section 2.2.

Image Analysis

Dendritic spines were assessed and counted as in section 2.2.

Spatial Analysis

Gained spine nearest neighbor analysis was conducted by measuring the distance from each spine gained during the learning phase of imaging to the nearest neighboring gained spine. Intervening stable, transient, or lost spines could exist between neighboring gained spines. Lost spine nearest neighbor analysis was conducted similarly, though for spines lost during the learning phase of imaging (e.g. the distance from a lost spine to its nearest neighboring lost spine was measured for all lost spines).

Clustered spine loss was assessed similar to clustered spine gain. The total number of spines that were lost within five or eight microns of each other during the learning phase was counted and divided by the total number of spines lost during the learning phase to calculate the percentage of clustered lost spines.

Several spatial measurements were taken for gained spine neighbor analysis. First, the distance between each new spine added during the learning phase and its nearest stable, pre-existing neighbor was measured in both trained and control animals. In trained animals, two further measurements were made; first, the distance from a new spine that was non-clustered to

its nearest neighbor, regardless of neighbor type (i.e. gained or stable), was assessed for all new, non-clustered spines. The same measurement was then made for new, clustered spines (i.e. the distance from each new, clustered spine to its nearest neighboring spine was measured). Spine type (i.e. new, clustered or pre-existing, stable) was also recorded for neighbors or clustered spines and utilized for the clustered to nearest neighbor analysis. Lost-to-gained nearest neighbor analysis was conducted by measuring the distance from each spine lost during the learning phase to its nearest gained neighbor spine. Spine type was also assessed for the gained neighbor (i.e. cluster or non-clustered).

Statistics

Correlations were calculated as Spearman's rho to compensate for the non-normality of the data. For analysis of distance between spines, the Kruskal-Wallis test was utilized. Variance was similar between groups for all comparisons. All p-values represent results from two-sided tests, $\alpha=0.05$. For analyses of the cumulative probability distributions of nearest neighbor measurements for gained spines and lost spines, the two-sample Kolmogorov-Smirnoff test was utilized. The Mann Whitney U-test was utilized for all other group comparisons.

3.3 Results

Spatial Distribution of Spine Gain and Loss

The cumulative probability distribution of nearest neighbor distance measurements between new spines added during the learning phase revealed a significant leftward shift toward smaller values for trained animals (Two-sample Kolmogorov-Smirnoff test, D=0.2740, p=5.74e-6) (Figure 3.1A). The average distance between two new spines was significantly smaller in trained animals (mean=8.189 μm, s.e.m.=0.886 μm) than control animals

(mean=13.585 µm, s.e.m.=1.209 µm) (Mann Whitney U-test, U=10299, p=0.0001) (Figure 3.1A,inset).

The cumulative probability distribution of nearest neighbor distance measurements between spines lost during the learning phase revealed a significant leftward shift toward smaller values for trained animals (Two-sample Kolmogorov-Smirnoff test, D=0.2160, p=9.5e-5) (Figure 3.1B). The average distance between two lost spines was significantly smaller in trained animals (mean=9.025 µm, s.e.m.=0.724 µm) than control animals (mean=13.488 µm, s.e.m.=0.914 µm) (Mann Whitney U-test, U=15969, p=0.0001) (Figure 3.1B, inset).

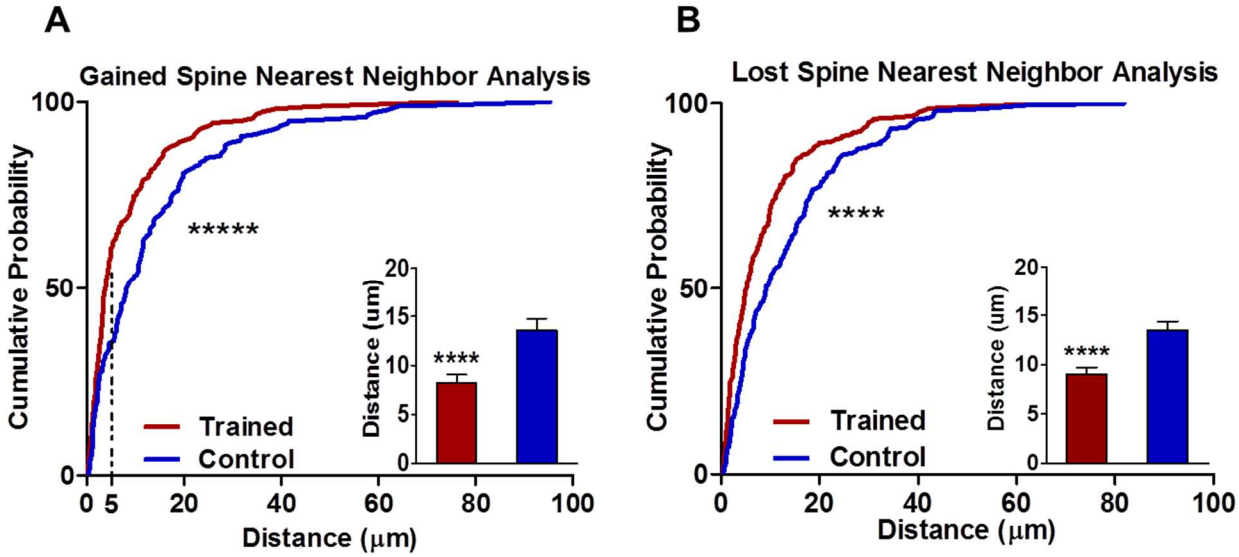

Figure 3.1: Learning shifts the spatial distribution of gained and lost spines.
(A) The cumulative probability distribution of the distance frome one new spine to its nearest neighboring new spine for trained animals was significantly shifted towards smaller values. (Trained, n=158 measurements; control, n=173 measurements). Inset is the mean ± s.e.m. of the values presented in the cumulative probability distribution. (B) The cumulative probability distribution of the distance from one lost spine to its nearest neighboring lost spine for trained animals was significantly shifted towards smaller values. (Trained, n=214 measurements; control, n=202 measurements). Inset is the mean ± s.e.m. of the values presented in the cumulative probability distribution. *****, p<0.00001, ****, p<0.0001. The 5 µm position is marked on (A).

Spatial Analysis of Clustered Spine Addition

New spines were preferentially added within 5 µm of each other when animals undergo a learning experience. Analysis of where new clustered and non-clustered spines occured relative to other spines revealed no difference between trained (mean=1.885 µm, s.e.m.=0.084

μm) and control (mean=1.799 μm, s.e.m.=0.074 μm) animals in the average distance between a new spine and the nearest pre-existing, stable neighboring spine (Dunn's multiple comparisons, p>0.05) (Figure 3.2A). Further, there was no difference between these distances and the average distance between new, non-clustered spines and their nearest neighbor, regardless of spine type (mean=1.789 μm, s.e.m.=0.100 μm) (Dunn's multiple comparisons, p>0.05) (Figure 3.2A). However, new, clustered spines had a significantly smaller average distance to their nearest neighboring spine, regardless of spine type (mean=1.193 μm, s.e.m.=0.063 μm) (Kruskal-Wallis test, Kruskal-Wallis statistic=32.74, p=0.0001) (Figure 3.2A).

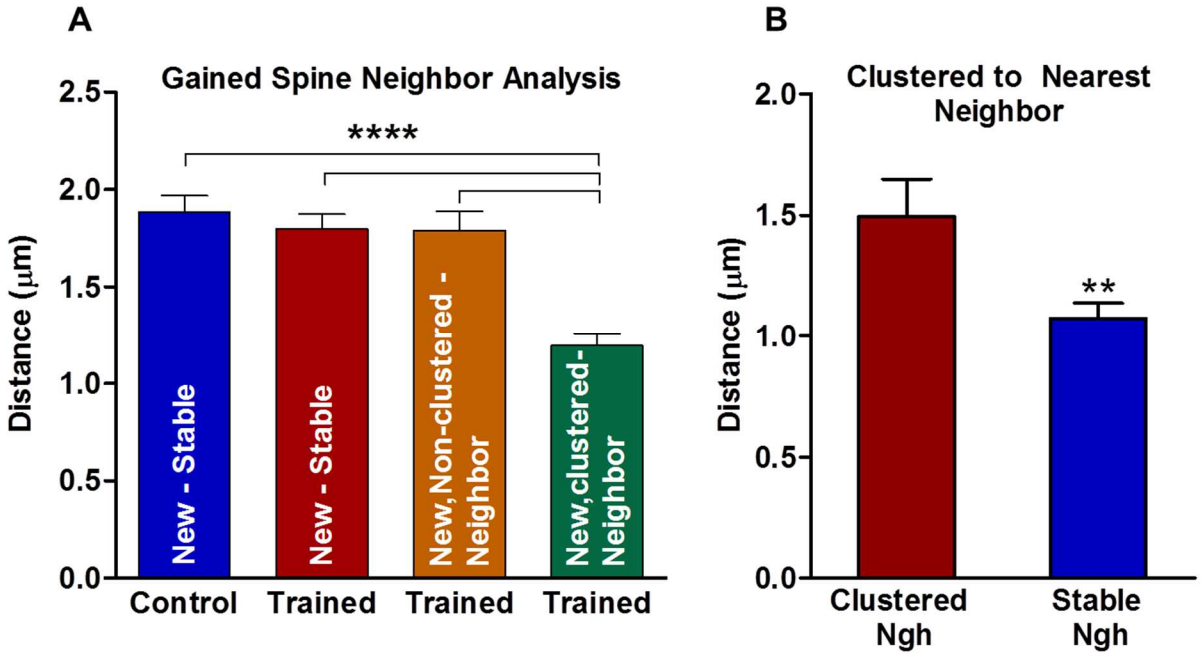

Figure 3.2: Spatial analysis of gained spines and neighboring spines.
(A) New spines added during the learning phase were not signicantly closer to stable spines in trained versus control animals (trained, n=381 measurements; control, n=385 measurements). Further, new, non-clustered spines in trained animals did not show a significant difference between the distance to the nearest neighboring spine – regardless of spine type – and the distance from new to stable spines (trained, new, non-clustered, n=211 measurements). Clustered, new spines added during learning in trained animals were significantly closer to their nearest neighboring spine (trained, new, clustered, n=147 measurements). (B) Analysis of neighboring spine type in trained animals revealed that new, clustered spines were significantly closer to neighboring stable spines than to neighboring new, clustered spines (clustered neighbors, n=41 measurements; stable neighbors, n=106 measurements). Ngh=neighbor. ****, p<.0001.

To asses if there was a bias in where new, clustered spines were added, we analyzed the nearest neighbor measurements by neighbor type. Strikingly, new, clustered spines were

on average added closer to existing, stable spines (mean= 1.075 µm, s.e.m.=0.062 µm) than to other new, clustered spines (mean=1.497 µm, s.e.m.=0.153 µm) (Mann Whitney, U=1571, p=0.0094) (Figure 3.2B).

Clustered Spine Loss

Analysis of clustered loss of spines was calculated using either an 8 µm window or the 5 µm window established for analysis of clustered spine addition. No significant difference in the percentage of spines lost in clusters existed between trained (mean=41.62%, s.e.m.=4.69%) and control (mean=31.05%, s.e.m.=4.30%) animals when utilizing a 8 µm window for clustering (Mann Whitney U-test, U=129.0, p=0.304) (Figure 3.3A). No significant difference in the percentage of spines lost in clusters existed between trained (mean=34.27%, s.e.m.=4.78%) and control (mean=21.61%, s.e.m.=3.61%) animals when utilizing a 5 µm window for clustering (Mann Whitney U-test, U=104.5, p=0.0711) (Figure 3.3B).

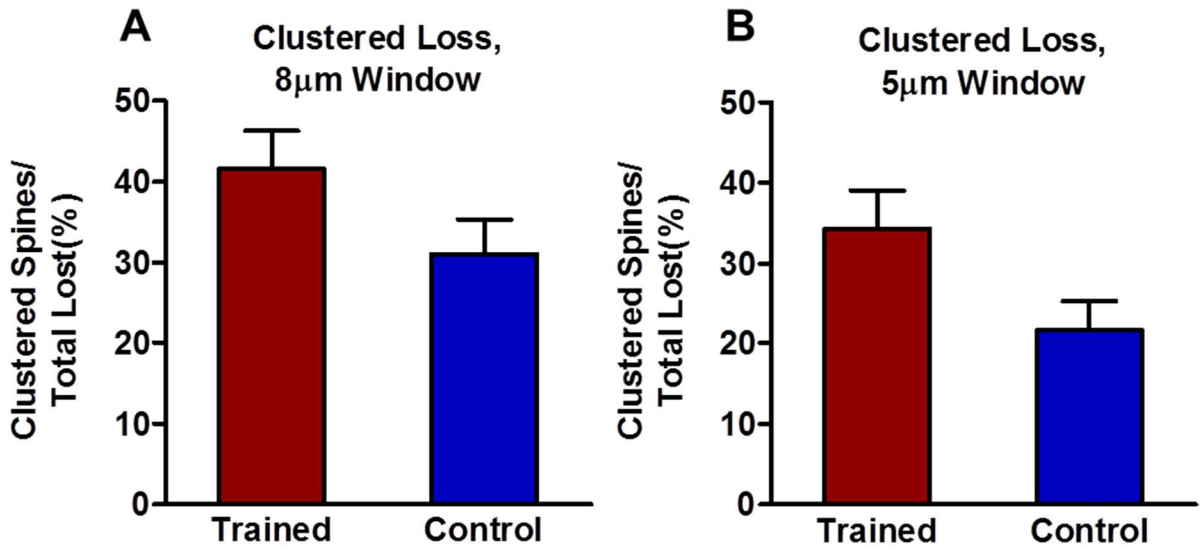

Figure 3.3: Clustered loss of dendritic spines.

(A) No difference existed between trained and control animals for the percentage of spines lost in clusters if an 8 µm window was used to assess for clustering. (B) No difference existed between trained and control animals for the percentage of spines lost in clusters if a 5 µm window was used to assess for clustering.

Behavioral Analysis of Spine Loss

While clustered spine addition during learning was strongly correlated with fear memory in contextually fear conditioned mice, we found no correlation to clustered spine loss. Utilizing an 8 μm window to assess clustering, there was no correlation between clustered spine loss during learning and average freezing behavior (Spearman's rho, r=0.417, p=0.086) (Figure 3.4A). Utilizing a 5 μm window for clustering revealed similar results, with a lack of correlation between clustered spine loss and average freezing (Spearman's rho, r=0.355, p=0.148) (Figure 3.4B).

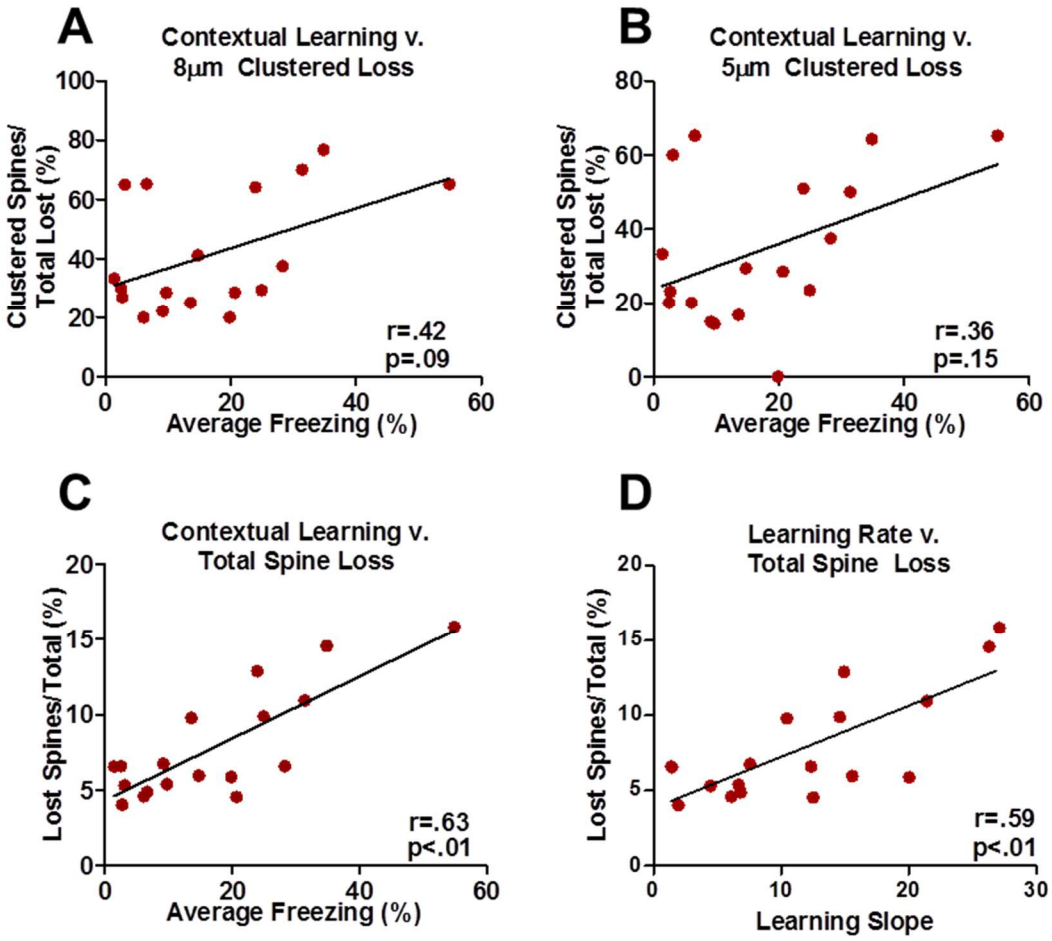

Figure 3.4: Behavorial analysis of spine loss during learning.

(A) No correlation existed between clustered spine loss assessed with an 8 μm clustering window and average freezing. (B) No correlation existed between clustered spine loss assessed with a 5 μm clustering window and average freezing. (C) Total spine loss during contextual fear conditioning was significantly correlated with average freezing. (D) Total spine loss also correlated to the rate of learning.

Strikingly, while no correlation between fear memory and clustered spine loss was observed, a significant correlation existed between both average freezing and total spine loss during learning (Spearman's rho, r=0.631, p=0.0050) (Figure 3.4C) and rate of learning and total spine loss (Spearman's rho, r=0.593, p=0.0094) (Figure 3.4D).

Spatial Analysis of Spine Gain and Loss

Spatial analysis separately of dendritic spine gain and loss revealed patterns to where spine dynamics occurred on a dendrite. We were thus interested to determine if gain and loss of spines exhibited a spatial interaction. In trained animals we found that the distance from a lost spine to its nearest gained neighboring spine was significantly smaller if the new spine was a clustered (mean=6.314 μm, s.e.m.=0.797 μm) versus non-clustered (mean=8.960 μm, s.e.m.=0.786 μm) new spine (Mann Whitney, U=9,850 , p=.014) (Figure 3.5A). To determine if there was a behaviorally relevant difference between spines lost near clustered new spines compared to non-clustered new spines, we plotted correlations to the percentage of spines lost in these groups to average freezing. We found that the proportion of spines lost within 5 μm of a clustered gained spine significantly correlated with average freezing (Spearman's rho, r=0.625, p=0.0056) (Figure 3.5B). However, we did not find a significant correlation between the percentage of spines lost within 5 μm of new, non-clustered spines and average freezing (Spearman's rho, r=-0.175, p=0.489) (Figure 3.5C).

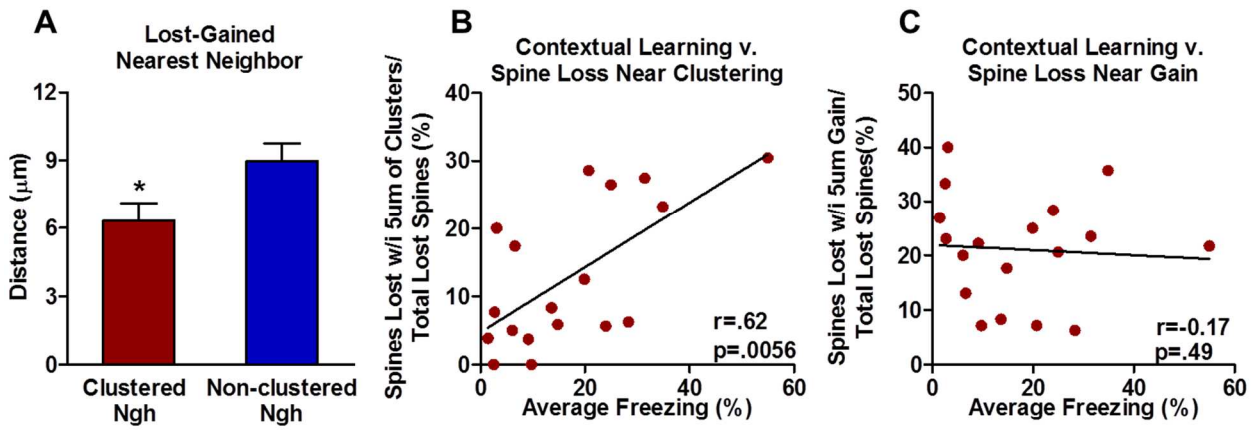

Figure 3.5: Spatial interaction of spine gain and loss during learning.
(A) Measurement of the distance between lost spines and their nearest neighboring gained spine revealed that lost spines were significantly closer to spines gained in clusters versus non-clustered gained spines (clustered neighbor, n=107 measurements; non-clustered neighbor, n=221 measurements). Ngh=neighbor. *, $p<0.05$.

3.4 Discussion

The finding that new spines were added in clusters within 5 μm of each other prompted a more general analysis of the spatial profile of spine dynamics. We found that the distribution of nearest neighbor distances between gained spines is significantly left-shifted toward smaller values in trained animals. Furthermore, the average nearest neighbor distance between gained spines is also significantly smaller in trained animals. These were not wholly unexpected results as a significantly larger percentage of new spines were already known to occur within 5 μm of each other. However, these findings demonstrate that spines in trained animals are more generally added near each, and suggest that for clustered spine addition molecular "crosstalk" occurring over distances of 5-10 μm may also interact with protein synthesis-dependent synaptic tag-and-capture mechanisms operating at distances up to 70 μm (Harvey and Svoboda, 2007; Harvey et al., 2008; Murakoshi et al., 2011; Govindarajan et al., 2011).

A more careful analysis of where new spines were added relative to existing spines revealed that clustered new spines were added significantly closer to their nearest neighbor in trained animals. This result is similar to the finding by Fu *et al* that clustered new spines were

added closer to neighboring spines in motor cortex following motor learning (Fu et al., 2012). When spine type of the neighboring spine was analyzed, we found that clustered new spines were added significantly closer to existing, stable spines. This result was novel and surprising and suggests that stable spines may serve as niduses around which new, clustered spines are added. One possible mechanism for this to occur is through the activation of nearby AMPA-silent synapses and subsequent spine growth due to NMDAR activation at stable spines (Winnubst and Lohmann, 2012).

The finding that the spatial distribution of spine gain was altered due to learning prompted an examination of the spatial profile of spine loss. We found that learning also caused a significant leftward shift of nearest neighbor distances measured between lost spines. This change was also reflected in a significant reduction in the average nearest neighbor distance between lost spines in trained animals. Spatially coordinated spine loss has been observed in hippocampal slice culture due to LTD inducing stimulation (Wiegert and Oertner, 2013). Here the authors utilized a window of 8 μm around a spine that had undergone LTD and found that neighboring spines within this region were more likely to be lost within 7 days of LTD induction. We thus assessed for clustered spine loss utilizing this 8 μm window and found no significant difference in the percentage of spines lost in clusters between trained and control animals. Similar findings were obtained if the window was narrowed to 5 μm, which had been used to assess for clustered spine gain. These results suggests that the spatial distribution of spine loss due to learning may not follow identical rules to that of spine gain and may be driven by different molecular interactions.

Behavioral assessment of spine loss revealed no significant correlation between fear and clustered loss with either the 8 μm or 5 μm window. Surprisingly, however, we did find a strong correlation between total spine loss during learning and fear memory assessed either as average freezing or as rate of learning. This result suggests that while clustered spine gain is important for learning, total spine loss may represent a more important structural change than

clustered loss of spines. Our finding, that spine loss in RSC correlated with fear learning in contextual fear conditioning, corroborates data from Lai *et al* showing spine loss due to tone fear conditioning occurred in frontal association cortex and correlated with freezing behavior (Lai et al., 2012).

Lai *et al* also showed a spatial interaction between spine loss during fear conditioning and spine gain due to fear extinction (Lai et al., 2012). The authors found that spines gained during fear extinction were less stable during subsequent tone fear re-conditioning if these spines existed within a narrow 2 μm window from the original site of spine loss. This suggests that gain and loss of spine may be coordinated by molecular cross talk operating over short distances. We tested our data for an interaction between spine loss and spine gain and found that lost spines were significantly closer to clustered, gained spines than to non-clustered, gained spines. This result supports the findings from Lai *et al* suggesting a spatial interaction between spine gain and loss. Our results also suggest that clustered new spines may consolidate molecular resources to a region of dendrite and promote coordination of spine dynamics more efficiently than non-clustered new spines.

To determine if a difference existed between the two populations of lost spines – those occurring near clustered spine gain and those occurring near non-clustered spine gain – we tested for behavioral effects. Specifically, we found a significant correlation between average freezing and the percentage of lost spines that occurred within 5 μm of a clustered new spine. Strikingly, we found no correlation between average freezing and the percentage of spines lost within 5 μm of a non-clustered, gained spine. Taken together, these results suggest a model where learning alters spine dynamics in a coordinated fashion at structural plasticity “hot spots” (Figure 3.6). Specifically, new spines relevant for learning are added near each other in clusters while spine loss related to learning occurs near the clustered spine addition.

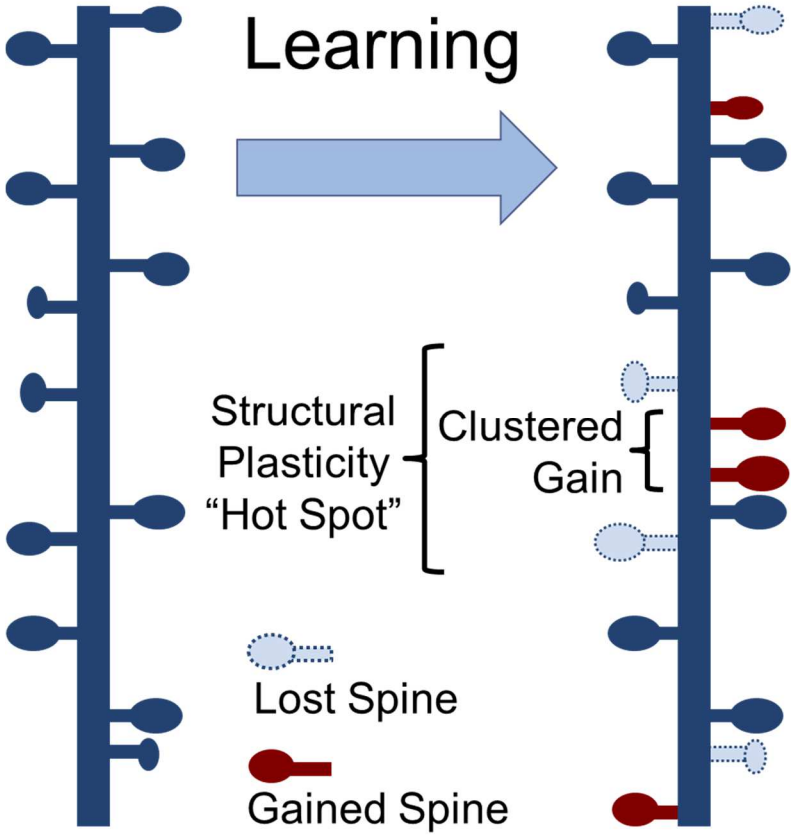

Figure 3.6: Model of Learning-related Structural Plasticity.
Structural plasticity following a learning event involves coordination of spine gain and spine loss at "hot spots" of plasticity. New spines relevant to learning are added near each other within clusters. Spine loss related to learning occurs near clustered spine addition.

3.5 References

Fu, M., Yu, X., Lu, J., & Zuo, Y. (2012). Repetitive motor learning induces coordinated formation of clustered dendritic spines in vivo. *Nature*, *483*(7387), 92–5.

Govindarajan, A., Israely, I., Huang, S.-Y., & Tonegawa, S. (2011). The Dendritic Branch Is the Preferred Integrative Unit for Protein Synthesis-Dependent LTP. *Neuron*, *69*(1), 132–146.

Govindarajan, A., Kelleher, R. J., & Tonegawa, S. (2006). A clustered plasticity model of long-term memory engrams. *Nature Reviews. Neuroscience*, *7*(7), 575–83.

Harvey, C. D., & Svoboda, K. (2007). Locally dynamic synaptic learning rules in pyramidal neuron dendrites. *Nature*, *450*(7173), 1195–200.

Harvey, C. D., Yasuda, R., Zhong, H., & Svoboda, K. (2008). The spread of Ras activity triggered by activation of a single dendritic spine. *Science (New York, N.Y.)*, *321*(5885), 136–40.

Lai, C. S. W., Franke, T. F., & Gan, W.-B. (2012). Opposite effects of fear conditioning and extinction on dendritic spine remodelling. *Nature*, *483*(7387), 87–91.

Murakoshi, H., Wang, H., & Yasuda, R. (2011). Local, persistent activation of Rho GTPases during plasticity of single dendritic spines. *Nature*, *472*(7341), 100–4.

Poirazi, P., & Mel, B. W. (2001). Impact of active dendrites and structural plasticity on the memory capacity of neural tissue. *Neuron*, *29*(3), 779–96.

Wiegert, J. S., & Oertner, T. G. (2013). Long-term depression triggers the selective elimination of weakly integrated synapses. *Proceedings of the National Academy of Sciences of the United States of America*, *110*(47), E4510–9.

Winnubst, J., & Lohmann, C. (2012). Synaptic clustering during development and learning: the why, when, and how. *Frontiers in Molecular Neuroscience*, *5*(May), 1–9.

Chapter 4

Spine Turnover before Training Predicts Future Learning and Learning-Related Spine Dynamics

4.1 Introduction

Turnover of dendritic spines is highest in young animals and wanes with maturity, though a baseline level persists throughout the life of an animal (Holtmaat et al., 2005; Zuo et al., 2005; Trachtenberg et al., 2002; Grutzendler et al., 2002; Majewska et al., 2006). Experience, sensory deprivation, and learning have all been shown to alter spine turnover in the adult (Jung and Herms, 2012; Zuo et al., 2005; Moczulska et al., 2013); and changes to spine dynamics during and after training have been shown to correlate with behavioral performance and/or memory (Xu et al., 2009, Lai et al., 2012). Strikingly, spine turnover before learning has also been shown to correlate with future performance (Roberts et al., 2010). Specifically, Roberts *et al* examined spine turnover in zebra finch HVC, a region critical for song learning, during animals' song learning critical period. The authors found that turnover in the days before song tutoring commenced positively correlated with future song acquisition. This result is exciting as few genetic of physiologic predictors of learning and memory have been discovered (Lee and Silva, 2009; Cohen-Matsliah et al., 2009; Ullman et al., 2014; Young et al., 2014; Saar and Barkai, 2009).

We found that contextual fear conditioning caused clustered gain and loss of spines and that these spine dynamics positively correlated with learning. Given the results of Roberts *et al* we were interested in assessing spine dynamics in RSC before learning. We sought to

determine if the findings from zebra finch during a critical period generalized to mammals in adulthood for episodic-like memory by examining spine gain and loss before commencement of contextual fear conditioning.

4.2 Methods

Surgery and Cranial Window Placement

Surgery and cranial window placement were conducted as in section 2.2.

Animals

The same animals imaged for spine dynamics in RSC from section 2.2 and 3.2 were utilized herein.

Behavioral Analysis

Animals were handled and contextually fear conditioned as in section 2.2. Assessment of freezing and calculation of average freezing and learning slope were conducted as in section 2.2.

Image Analysis

Dendritic spines were assessed and counted as in section 2.2. Baseline turnover was calculated as the total number of spines gained between baseline 1 and baseline 2 added to the total number of spines lost between baseline 1 and baseline 2, divided by twice the total number of spines present on baseline 1 ((Spines gained BL1-BL2 + Spines lost BL1-BL2)/(2*Total spines on BL1)).

Statistics

Correlations were calculated as Spearman's rho to compensate for the non-normality of the data. The Mann Whitney U-test was utilized for all other group comparisons. All p-values represent results from two-sided tests, $\alpha=0.05$.

4.3 Results

Baseline Spine Turnover, Fear Learning, and Spine Clustering

Turnover of spines before commencement of the learning phase, referred to as baseline spine turnover, was calculated as the total gain and loss of spines over this time period divided by twice the total number of spines counted on the first imaging day (baseline 1) (the total number of spines is doubled to account for the inclusion of both gain and loss in this calculation). We found no significant difference in the rate of spine turnover between trained (mean=4.420%, s.e.m.=0.376%) and control (mean=4.508%, s.e.m.=0.738%) animals at baseline (Mann Whitney, U=143.0, p=0.558) (Figure 4.1A). Furthermore, no significant difference in spine turnover existed during the learning phase between animals undergoing contextual fear conditioning (mean=6.909%, s.e.m.=0.691%) and home cage controls (mean=6.976%, s.e.m.=1.015%) (Mann Whitney, U=158.0, p=0.912). (Figure 4.1B). Spine turnover was higher during the learning phase for both trained and control animals as the window over which gain and loss was assessed was larger during the learning phase (2 days for baseline turnover and 5 days for learning phase turnover).

To assess for an impact of baseline spine turnover on learning, we correlated future contextual fear learning with baseline spine turnover. We found a significant correlation between future learning, assessed as average freezing, with spine turnover before commencement of training (Spearman's rho, r=0.548, p=0.019) (Figure 4.1C).

To test if baseline gain and loss of spines is related to spine dynamics during the learning phase, we correlated baseline spine turnover with the clustered addition of new spines. We found a significant positive correlation between baseline spine turnover and future spine clustering during contextual fear conditioning (Spearman's rho, r=0.576, p=0.012) (Figure 4.1D).

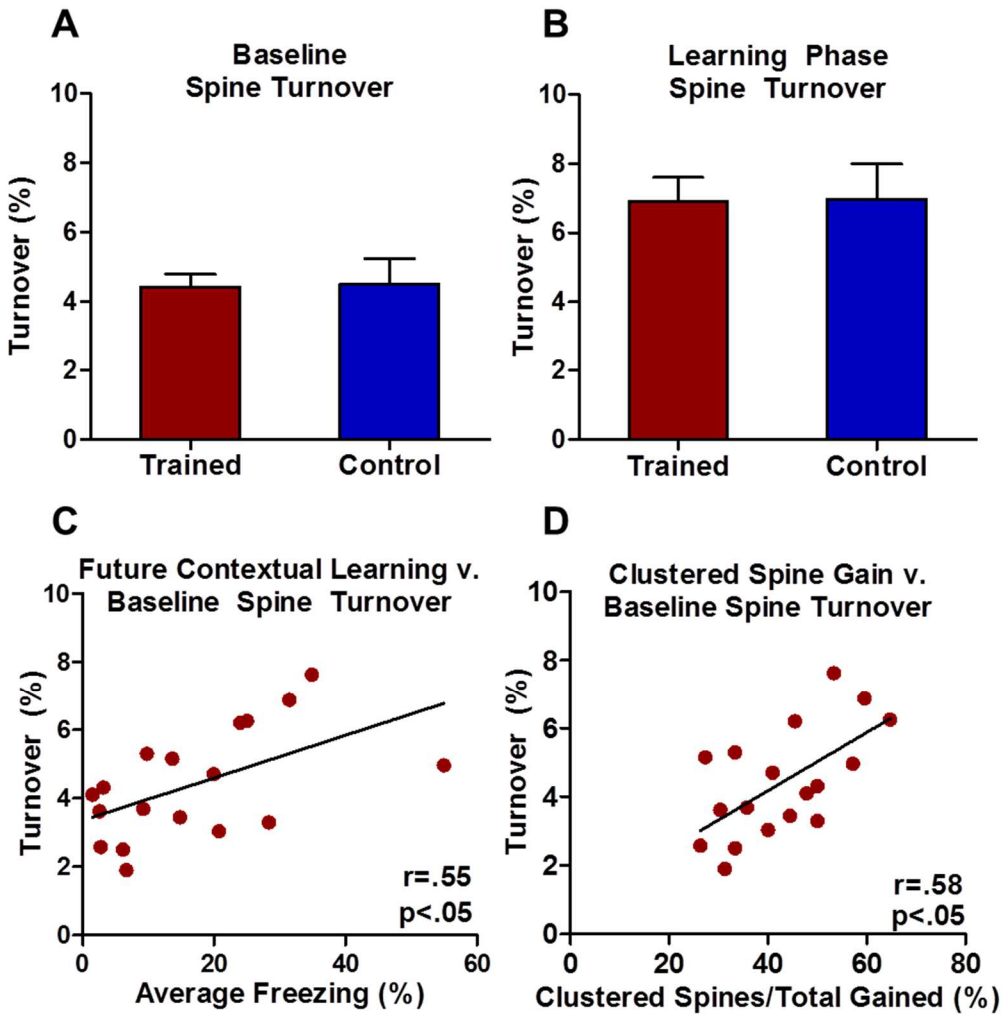

Figure 4.1: Baseline Spine turnover correlates with learning.
(A) Average spine turnover before the learning phase (i.e. while all animals have only experienced the home cage) did not differ between animals who remained home cage controls (control, n=18 mice) and animals who underwent contextual fear conditioning (trained, n=18 mice). (B) Average spine turnover during the learning phase did not differ between animals who underwent contextual fear conditioning (trained, n=18 mice) and home cage controls (control, n=18 mice). Turnover during learning was higher than during baseline as the interval over which spine gain and loss was assessed was larger (2 days during baseline and 5 days during learning). (C) In trained animals, spine turnover before learning correlated with future contextual learning assessed as average freezing. (D) Clustered addition of spines during contextual fear learning correlated with baseline turnover of spines before commencement of training.

4.4 Discussion

Previous results from zebra finch suggested that turnover of spines immediately prior to learning correlated to future learning (Roberts et al., 2010). These results were novel as few features of the physiologic or genetic state of an animal before learning have been shown to

have predictive value as to how well an animal will learn (Lee and Silva, 2009; Cohen-Matsliah et al., 2009; Ullman et al., 2014; Young et al., 2014; Saar and Barkai, 2009). For example, loss of thin spines in dorsolateral prefrontal cortex of aged rhesus monkeys was shown to correlate with a decrease in performance on a delayed nonmatching- to-sample working memory task (Young et al., 2014). Conversely, environmental enrichment is shown to both enhance spine turnover and enhance contextual fear conditioning as well as novel object recognition memory (Bednarek and Caroni, 2011). Further, a number of studies have shown an enhancement in intrinsic excitability of pyramidal neurons in piriform cortex that correlates with rats' ability to learn and perform olfactory discrimination tasks (Saar et al., 1998; Cohen-Matsliah et al., 2009; Saar and Barkai, 2009). Finally, a number of genes have been discovered that enhance learning in mice when either knocked out or overexpressed (Lee and Silva, 2009).

The findings from Roberts *et al* may reflect a unique state of spine dynamics that occurs only in the critical period for song learning in zebra finch; this is to say that critical period learning and the associated structural plasticity may be unique from learning and memory during adulthood and in mammals. We thus sought to test the findings of Roberts *et al* in a mammalian system and in the adult animal. We found that spine turnover in adult mouse RSC in the days prior to commencement of contextual fear conditioning positively correlated with future contextual learning. This corroborated and extended the findings of Roberts *et al* by demonstrating that structural dynamics before learning in adult mammals are predictive of future learning, suggesting that spine turnover in the critical period may serve a similar function as spine turnover in the adult.

We did not find a change in spine turnover during the learning phase of imaging between animals undergoing contextual fear conditioning and home cage control animals. This result supported our finding that spine gain and loss measured between each imaging day did not differ significantly between experimental groups. However, Roberts *et al* found a significant difference in turnover immediately following learning, which they attributed to a spine stabilizing

property of learning. Our data do support this idea: animals trained in contextual fear conditioning had an increased percentage of new spines added in clusters and clustered new spines were more stable than non-clustered new spines. We further found that baseline turnover positively correlated with future spine clustering. Roberts *et al* did not assess for clustered spine addition during learning, but our results suggest that learning generally serves to stabilize spines involved in memory formation, and one mechanism by which this is accomplished is clustered spine formation.

We suggest a model that integrates results of Roberts *et al* and Bednarek and Caroni: Roberts *et al* demonstrate that individual animals have variability in baseline spine turnover and that higher levels of turnover correlate with improved learning (Roberts et al., 2010); Bednarek and Caroni show that manipulations, such as environmental enrichment, that enhance spine turnover are able to enhance learning (Bednarek and Caroni, 2011). Based on predictions from Caroni *et al*, we suggest that increased dendritic spine turnover increases the rate at which a given neuron samples the potential synaptic connectivity space around it (Caroni et al., 2014). Thus, neurons with higher sampling rates are better able to make connections that are functionally important for learning. When relevant connections are made, they are stabilized by clustered addition of spines at this location.

4.5 References

Bednarek, E., & Caroni, P. (2011). β-Adducin Is Required for Stable Assembly of New Synapses and Improved Memory Upon Environmental Enrichment. *Neuron*, *69*(6), 1132–1146.

Caroni, P., Chowdhury, A., & Lahr, M. (2014). Synapse rearrangements upon learning: from divergent–sparse connectivity to dedicated sub-circuits. *Trends in Neurosciences*, *37*(10), 604–614.

Cohen-Matsliah, S. I., Rosenblum, K., & Barkai, E. (2009). Olfactory-learning abilities are correlated with the rate by which intrinsic neuronal excitability is modulated in the piriform cortex. *European Journal of Neuroscience*, *30*(July), 1339–1348.

Grutzendler, J., Kasthuri, N., & Gan, W.-B. (2002). Long-term dendritic spine stability in the adult cortex. *Nature*, *420*(6917), 812–6.

Holtmaat, A. J. G. D., Trachtenberg, J. T., Wilbrecht, L., Shepherd, G. M., Zhang, X., Knott, G. W., & Svoboda, K. (2005). Transient and persistent dendritic spines in the neocortex in vivo. *Neuron*, *45*(2), 279–91.

Jung, C. K. E., & Herms, J. (2012). Structural Dynamics of Dendritic Spines are Influenced by an Environmental Enrichment: An In Vivo Imaging Study. *Cerebral Cortex (New York, N.Y. : 1991)*, *24*, 377–384.

Lai, C. S. W., Franke, T. F., & Gan, W.-B. (2012). Opposite effects of fear conditioning and extinction on dendritic spine remodelling. *Nature*, *483*(7387), 87–91.

Lee, Y.-S., & Silva, A. J. (2009). The molecular and cellular biology of enhanced cognition. *Nat Rev Neurosci*, *10*(2), 126–140.

Majewska, A. K., Newton, J. R., & Sur, M. (2006). Remodeling of synaptic structure in sensory cortical areas in vivo. *The Journal of Neuroscience : The Official Journal of the Society for Neuroscience*, *26*(11), 3021–3029.

Moczulska, K. E., Tinter-Thiede, J., Peter, M., Ushakova, L., Wernle, T., Bathellier, B., & Rumpel, S. (2013). Dynamics of dendritic spines in the mouse auditory cortex during memory formation and memory recall. *Proceedings of the National Academy of Sciences of the United States of America*, *110*(45), 18315–20.

Roberts, T. F., Tschida, K. A., Klein, M. E., & Mooney, R. (2010). Rapid spine stabilization and synaptic enhancement at the onset of behavioural learning. *Nature*, *463*(7283), 948–52.

Saar, D., & Barkai, E. (2009). Long-lasting maintenance of learning-induced enhanced neuronal excitability: Mechanisms and functional significance. *Molecular Neurobiology*, *39*(3), 171–177.

Saar, D., Grossman, Y., & Barkai, E. (1998). Reduced after-hyperpolarization in rat piriform cortex pyramidal neurons is associated with increased learning capability during operant conditioning. *European Journal of Neuroscience*, *10*(4), 1518–1523.

Trachtenberg, J. T., Chen, B. E., Knott, G. W., Feng, G. P., Sanes, J. R., Welker, E., & Svoboda, K. (2002). Long-term in vivo imaging of experience-dependent synaptic plasticity in adult cortex. *Nature*, *420*(6917), 788–794.

Ullman, H., Almeida, R., & Klingberg, T. (2014). Structural maturation and brain activity predict future working memory capacity during childhood development. *The Journal of Neuroscience : The Official Journal of the Society for Neuroscience*, *34*(5), 1592–8.

Xu, T., Yu, X., Perlik, A. J., Tobin, W. F., Zweig, J. a, Tennant, K., … Zuo, Y. (2009). Rapid formation and selective stabilization of synapses for enduring motor memories. *Nature*, *462*(7275), 915–9.

Young, M. E., Ohm, D. T., Dumitriu, D., Rapp, P. R., & Morrison, J. H. (2014). Differential effects of aging on dendritic spines in visual cortex and prefrontal cortex of the rhesus monkey. *Neuroscience*, *274*, 33–43.

Zuo, Y., Lin, A., Chang, P., & Gan, W.-B. (2005). Development of long-term dendritic spine stability in diverse regions of cerebral cortex. *Neuron*, *46*(2), 181–9.

Chapter 5

Conclusions

5.1 Integration of Results

The clustered plasticity hypothesis states that plastic changes are not randomly distributed, but rather are grouped together in functionally relevant clusters. Convergent support for this hypothesis comes from biochemical studies of local interactions between dendritic spines undergoing LTP, electrophysiological studies of spatiotemporally correlated synaptic inputs, computational studies of information storage in clustered neurons, and structural studies of clustered spine addition following learning. To further explore clustered plasticity, I utilized chronic *in vivo* two-photon fluorescence microscopy to track dendritic spine dynamics in the RSC of mice as they underwent contextual fear conditioning. This approach allowed us to determine if clustered structural plasticity observed in primary motor cortex due to motor learning (Fu et al., 2012) was generalizable to other cortical regions and other memory systems.

The results of this thesis corroborate and extend the existing convergent evidence for clustered plasticity by finding clustered spine addition in RSC during contextual fear conditioning. This suggests that clustered addition of dendritic spines is a fundamental mechanism used for information storage in the mouse brain. The finding of spine clustering in both barn owl (McBride et al., 2008) and mouse (Fu et al., 2012) suggest this finding is a feature that also spans taxonomic class. While chronic *in vivo* imaging of spines has not been conducted in primates, evidence for clustering of spines has been found in rhesus monkey

prefrontal cortex (Yadav et al., 2012). Here the authors identified all spines on layer 3 neurons from fixed tissue samples and utilized a novel clustering algorithm paired with Monte Carlo simulation to demonstrate spatial clustering of spines. As a whole, these results suggest that spine clustering occurs in a variety of species, in a variety of cortical regions, and as a result of a variety of learning and memory paradigms, truly suggesting that this is a fundamental mechanism for information storage.

A detailed spatial analysis of spine dynamics in mouse RSC revealed that contextual fear conditioning also altered where spine loss occurred. In trained animals we found that spines were lost closer to each other, though not in a strictly clustered fashion. Excitingly, spines lost following contextual fear conditioning were also found to be lost closer to clustered new spines. While spine loss due to learning had been shown to occur near spine gain (Lai et al., 2012), we believe this is the first example of coordination between clustered spine gain and spine loss. These findings suggest that clustered gain of spines is balanced by loss of nearby spines, potentially disrupting pre-existing spine clusters. We propose a model of spine dynamics where learning-related structural changes occur in plasticity “hot spots” which represent spatially restricted regions of clustered spine gain balanced by spine loss.

Excitingly, our design allowed us to examine if spine dynamics purported to occur as a result of learning had any correlation to behavioral readouts of learning and memory. Our finding that clustered addition of new spines during contextual fear conditioning positively and linearly correlated with freezing behavior is the first example of a correlation between dendritic spine clustering and behavior. Additionally, we found that total spine loss correlated to behavior; but a further examination of this data revealed that spine loss within 5 μm of clustered new spines correlated with learning but spine loss occurring within 5 μm of non-clustered new spines did not. This finding supported the idea of plasticity “hot spots” where functionally related and behaviorally relevant spine dynamics occur in a spatially clustered manner.

Given the findings of Roberts *et al*, we were interested in how the basal state of the adult cortex may influence the ability of an animal to integrate new information (Roberts et al., 2010). We addressed this question by examining spine dynamics in the days before commencement of contextual fear conditioning. Our finding that baseline spine turnover correlated with future learning supports the findings of Roberts *et al* that spine turnover in zebra finch HVC correlated with future song learning. Our results further suggest that spine turnover is a more generalized predictor of learning ability and not a specialized property of the zebra finch HVC or of critical period learning. We thus suggest that spine turnover represents a generalized ability of neurons to sample their synaptic space for potential connections: higher turnover equates with a higher sampling rate and an increase in the likelihood of the creation of relevant connections. When important connections are established one mechanism suggested by our data to stabilize these new spines is by clustered spine addition.

5.2 Future Directions

The results of this thesis establish the mouse RSC as an excellent model system in which to study dendritic spine dynamics at baseline and during spatial learning. The initial findings of clustered spine addition, spatially coordinated spine loss, and correlations for both of these measures to behavior are exciting and novel and make further predications that could be tested in the future. Further, biochemical and electrophysiological studies of clustered plasticity suggest a number of future studies which could be conducted in mouse RSC.

Several broad areas of study could be explored by utilizing the RSC as a model to study clustered plasticity. First, examination of clustered spine addition in RSC could be explored utilizing a different spatial learning task. For instance, mice could be trained on the Morris Water maze, a task known to involve RSC (Czajkowski et al., 2014). Finding clustered spine addition due to training in this task would add support to the notion that clustered structural

plasticity is relevant for learning and is not simply an epiphenomenon of contextual fear conditioning. This finding would also add support for an involvement of RSC in spatial learning in Morris water maze.

A related set of experiments could manipulate learning to test for changes to spine clustering. Utilizing a mouse with a genetic mutation that enhances learning might be expected to enhance the percentage of new spines that are added in clusters. Conversely, utilizing a mouse with a mutation that suppresses learning might be expected to reduce the percentage of clustered spines. Both of these results would provide convergent evidence that spine clustering and contextual learning are importantly related. Finally, one could manipulate the context memory established by contextual fear conditioning, perhaps by conducting extinction training, and monitor changes to spine clusters. One may expect that clustered spines established during fear condition are lost during extinction, similar to the results of Lai *et al* (Lai et al., 2012).

Two important and related questions left unanswered by our current results are how clustered new spines relate to each other functionally and how they relate to contextual learning. There are two related aspects to the first question: 1) do clustered spines receive similar inputs and are thus co-activated, and 2) do clustered spines share the same presynaptic partner? The first question could be addressed by utilizing genetically encoded calcium indicators, such as the GCaMP family of fluorescent proteins, to track neuronal activity (Badura et al., 2014). In fact, a Thy1-GCaMP transgenic mouse was created recently and shown to sparsely express GCaMP in apical dendrites and dendritic spines of layer 5 pyramidal neurons (Chen et al., 2012). To mark structure, sparse labeling with a lentiviral vector modified to express a red fluorescent protein would be injected into Thy1-GCaMP mice during cranial window implantation. Utilizing an air-lifted platform and head fixation (Kislin et al., 2014) we could conduct awake *in vivo* two-photon imaging during contextual fear conditioning and track dendrite and dendritic spine activity. Following conditioning, animals could be maintained on the microscope to gather structural data. Structural analysis of spine gain and loss would be

conducted as in this thesis, but could then be correlated to neuronal activity that occurred during contextual conditioning. While it is possible that new clustered spines are not functionally related, results from Takahashi *et al* suggest we would find co-activity of clustered spines (Takahashi et al., 2012). Further, models of the establishment of spine clustering suggest co-activity of new spines may be a requirement for stabilization of these structures (DeBello, 2008; DeBello et al., 2014). Furthermore, analysis of neuronal activity correlated to the behavior of the animal during fear conditioning would also allow us to address the issue of the relevancy of spine clustering to learning. While are data suggest clustered spine addition is an important mechanism for contextual fear conditioning, it is possible spine clustering is epiphenomenal to learning. By tracking neuronal activity during behavior and learning we could better address this issue.

The second aspect to the question of the functional relationship between clustered spines is how they are anatomically wired with respect to each other. Do new clustered spines share the same presynaptic bouton, as suggested by the appearance of multi-spine boutons in CA1 following LTP induction (Toni et al., 1999)? Alternatively, clustered new spines may have entirely unique presynaptic partners. To address this question we could utilize EM reconstruction of identified clustered spines to assess presynaptic partnership (Trachtenberg et al., 2002; Knott et al., 2009).

Finally, the properties of clustered plasticity could be more thoroughly explored in the RSC-contextual fear conditioning model herein established. For example, Govindarajan *et al* show a partial blockade of sharing of plasticity-related proteins across dendritic branch points (Govindarajan et al., 2011). This suggests that individual dendritic branches may serve as computational units, and one might then expect clustering to be established in a branch-specific manner. This could be tested by tracing the entire dendritic arbor of a given neuron and assessing for an equal distribution of clustered spines across all branches or a biased distribution of clustering to select branches. Combining this analysis with GCaMP-mediated

calcium imaging would also allow for an exploration of the electrical properties of individual branches that facilitate or inhibit clustered spine formation.

Finally, a detailed analysis of the plasticity "hot spot" is warranted. Imaging of the full dendritic arbor would allow us to determine the spatial distribution of "hot spots" across the entire dendritic field of a given neuron. It is likely that the "hot spot" would follow a similar spatial distribution as clustered spines and show a preference for specific branches. In this case we could assess for the spatial distribution of "hot spots" along a given branch. This is would allow us to determine if this is a "clustering of clustering" such that "hot spots" also show a structured spatial arrangement. Additionally, assessment of where (i.e. proximal versus distal dendrites) within the dendritic tree "hot spots" occur has important implications for how these structures might be used in computations (Arrigoni and Greene, 2004; Spruston, 2008; Behabadi et al., 2012; Medinilla et al., 2013). Furthermore, a larger sampling of dendritic plasticity "hot spots" would allow us to better characterize their size, shape, and composition, time course of appearance and disappearance, and relationship to behavior.

5.3 References

Arrigoni, E., & Greene, R. W. (2004). Schaffer collateral and perforant path inputs activate different subtypes of NMDA receptors on the same CA1 pyramidal cell. *British Journal of Pharmacology*, *142*(2), 317–322.

Badura, A., Sun, X. R., Giovannucci, A., Lynch, L. A., & Wang, S. S.-H. (2014). Fast calcium sensor proteins for monitoring neural activity. *Neurophotonics*, *1*(2), 025008.

Behabadi, B. F., Polsky, A., Jadi, M., Schiller, J., & Mel, B. W. (2012). Location-dependent excitatory synaptic interactions in pyramidal neuron dendrites. *PLoS Computational Biology*, *8*(7), 40–42.

Chen, Q., Cichon, J., Wang, W., Qiu, L., Lee, S. J. R., Campbell, N. R., … Feng, G. (2012). Imaging Neural Activity Using Thy1-GCaMP Transgenic Mice. *Neuron*, *76*(017892), 297–308.

Czajkowski, R., Jayaprakash, B., Wiltgen, B., Rogerson, T., Guzman-Karlsson, M. C., Barth, A. L., Trachtenberg, J., Silva, A. J. (2014). Encoding and storage of spatial information in

the retrosplenial cortex. *Proceedings of the National Academy of Sciences of the United States of America*, *111*(23), 8661–6.

DeBello, W. M. (2008). Micro-rewiring as a substrate for learning. *Trends in Neurosciences*, *31*(11), 577–84.

DeBello, W. M., McBride, T. J., Nichols, G. S., Pannoni, K. E., Sanculi, D., & Totten, D. J. (2014). Input clustering and the microscale structure of local circuits. *Frontiers in Neural Circuits*, *8*(September), 112.

Fu, M., Yu, X., Lu, J., & Zuo, Y. (2012). Repetitive motor learning induces coordinated formation of clustered dendritic spines in vivo. *Nature*, *483*(7387), 92–5.

Govindarajan, A., Israely, I., Huang, S.-Y., & Tonegawa, S. (2011). The Dendritic Branch Is the Preferred Integrative Unit for Protein Synthesis-Dependent LTP. *Neuron*, *69*(1), 132–146.

Kislin, M., Mugantseva, E., Molotkov, D., Kulesskaya, N., Khirug, S., Kirilkin, I., … Khiroug, L. (2014). Flat-floored Air-lifted Platform: A New Method for Combining Behavior with Microscopy or Electrophysiology on Awake Freely Moving Rodents. *Journal of Visualized Experiments : JoVE*, 1–11.

Knott, G. W., Holtmaat, A., Trachtenberg, J. T., Svoboda, K., & Welker, E. (2009). A protocol for preparing GFP-labeled neurons previously imaged in vivo and in slice preparations for light and electron microscopic analysis. *Nature Protocols*, *4*(8), 1145–56.

Lai, C. S. W., Franke, T. F., & Gan, W.-B. (2012). Opposite effects of fear conditioning and extinction on dendritic spine remodelling. *Nature*, *483*(7387), 87–91.

McBride, T. J., Rodriguez-Contreras, A., Trinh, A., Bailey, R., & Debello, W. M. (2008). Learning drives differential clustering of axodendritic contacts in the barn owl auditory system. *The Journal of Neuroscience : The Official Journal of the Society for Neuroscience*, *28*(27), 6960–73.

Medinilla, V., Johnson, O., & Gasparini, S. (2013). Features of proximal and distal excitatory synaptic inputs to layer V neurons of the rat medial entorhinal cortex. *The Journal of Physiology*, *591*(Pt 1), 169–83.

Roberts, T. F., Tschida, K. A., Klein, M. E., & Mooney, R. (2010). Rapid spine stabilization and synaptic enhancement at the onset of behavioural learning. *Nature*, *463*(7283), 948–52.

Spruston, N. (2008). Pyramidal neurons: dendritic structure and synaptic integration. *Nature Reviews. Neuroscience*, *9*(3), 206–21.

Takahashi, N., Kitamura, K., Matsuo, N., Mayford, M., Kano, M., Matsuki, N., & Ikegaya, Y. (2012). Locally Synchronized Synaptic Inputs. *Science*, *335*(6066), 353–356.

Toni, N., Buchs, P., Nikonenko, I., & Bron, C. (1999). LTP promotes formation of multiple spine synapses between a single axon terminal and a dendrite. *Nature*, *402*(November), 421–425.

Trachtenberg, J. T., Chen, B. E., Knott, G. W., Feng, G. P., Sanes, J. R., Welker, E., & Svoboda, K. (2002). Long-term in vivo imaging of experience-dependent synaptic plasticity in adult cortex. *Nature*, *420*(6917), 788–794.

Yadav, A., Gao, Y. Z., Rodriguez, A., Dickstein, D. L., Wearne, S. L., Luebke, J. I., … Weaver, C. M. (2012). Morphologic evidence for spatially clustered spines in apical dendrites of monkey neocortical pyramidal cells. *The Journal of Comparative Neurology*, *520*(13), 2888–902.